

**THE SYSTEMATIC AND RANDOM ERRORS
DETERMINATION USING REAL-TIME 3D SURFACE
TRACKING SYSTEM IN BREAST CANCER**

JARUEK KANPHET

**A THESIS SUBMITTED IN PARTIAL FULFILLMENT
OF THE REQUIRMENT FOR
THE DEGREE OF MASTER OF SCIENCE
(MEDICAL PHYSICS)
FACULTY OF GRADUATE STUDIES
MAHIDOL UNIVERSITY
2016**

COPYRIGHT OF MAHIDOL UNIVERSITY

Thesis
entitled
**THE SYSTEMATIC AND RANDOM ERRORS
DETERMINATION USING REAL-TIME 3D SURFACE
TRACKING SYSTEM IN BREAST CANCER**

Jaruek Kanphet

.....
Mr. Jaruek Kanphet
Candidate

Nuanpen Das

.....
Lect. Nuanpen Dumrongkijudom,
Ph.D. (Medical Radiation Physics)
Major advisor

Taweap Sanghangthum

.....
Mr. Taweap Sanghangthum,
Ph.D. (Nuclear Engineering)
Co-advisor

Patcharee Lertrit

.....
Prof. Patcharee Lertrit,
M.D., Ph.D. (Biochemistry)
Dean
Faculty of Graduate Studies
Mahidol University

Puangpen Tangboonduangjit

.....
Lect. Puangpen Tangboonduangjit,
Ph.D. (Medical Radiation Physics)
Program Director
Master of Science Program in
Medical Physics
Faculty of Medicine
Ramathibodi Hospital
Mahidol University

Thesis
entitled
**THE SYSTEMATIC AND RANDOM ERRORS DETERMINATION
USING REAL-TIME 3D SURFACE TRACKING SYSTEM IN
BREAST CANCER**

was submitted to the Faculty of Graduate Studies, Mahidol University
for the degree of Master of Science (Medical Physics)

on
May 12, 2016

Jaruek Kanphet
.....
Mr. Jaruek Kanphet
Candidate

Sivalee Suriyapee
.....
Assoc. Prof. Sivalee Suriyapee,
M.eg (Nuclear Engineering)
Chair

Nuanpen Dumrongkijudom
.....
Lect. Nuanpen Dumrongkijudom,
Ph.D. (Medical Radiation Physics)
Member

Taweap Sanghangthum
.....
Mr. Taweap Sanghangthum,
Ph.D. (Nuclear Engineering)
Member

Puangpen Tangboonduangjit
.....
Lect. Puangpen Tangboonduangjit,
Ph.D. (Medical Radiation Physics)
Member

Patcharee Lertrit
.....
Prof. Patcharee Lertrit,
M.D., Ph.D. (Biochemistry)
Dean
Faculty of Graduate Studies
Mahidol University

Piyamitr Sritara
.....
Prof. Piyamitr Sritara,
M.D., FRCPT, FACP, FRCP
Dean
Faculty of Medicine
Ramathibodi Hospital
Mahidol University

ACKNOWLEDGEMENTS

I would like to express my sincere gratitude and deepest appreciation to my major advisor, Dr. Nuanpen Dumrongkijudom, Department of Radio Technology, Faculty of Medical Technology, Mahidol University and my co-advisor, Dr. Taweap Sanghangthum, Physicist at Division of Therapeutic Radiology and Oncology, Department of Radiology, King Chulalongkorn Memorial Hospital, for their guidance, invaluable advice, supervision, constructive comments and English language proof in this thesis.

I would like to deeply thank to my thesis committee, Ass. Prof. Sivalee Suriyapee, Chief Physicist at Division of Therapeutic Radiology and Oncology, Department of Radiology, Faculty of Medicine, Chulalongkorn University, for her knowledge, patience, motivation, enthusiasm, and her kindness in examining the research methodology and provide suggestion for the improvement.

I would like to thank Dr. Puangpen Tangboonduangjit, Department of Radiology, Faculty of Medicine, Ramathibodi Hospital, Mahidol University for her suggestion and constructive comment in this research.

I am grateful to all physicist and technologist at Division of Therapeutic Radiology and Oncology, Department of Radiology, King Chulalongkorn Memorial Hospital and all teacher, lecturers and staff in Master Science Program in Medical Physics, Faculty of Medicine, Ramathibodi Hospital for their kind support and supply the knowledge in Medical Physics.

This research is partially supported by Graduate Studies of Mahidol University Alumni Association that I would like to thank.

Finally, I am grateful to my family for their financial support and understanding during the entire course of study.

Jaruek Kanphet

THE SYSTEMATIC AND RANDOM ERRORS DETERMINATION USING REAL-TIME 3D SURFACE TRACKING SYSTEM IN BREAST CANCER

JARUEK KANPHET 5637832 RAMP/M

M.Sc. (MEDICAL PHYSICS)

THESIS ADVISORY COMMITTEE: NUANPEN DUMRONGKIJUDOM, Ph.D. TAWEAP SANGHANGYHUM, Ph.D.

ABSTRACT

In advanced radiotherapy, the modern technologies and new techniques are used to improve the potential of cancer treatment. The IGRT was applied to verify tumor's position before treatment. The use of IGRT is possible to reduce dose and side effects to normal tissues and increase the dose to the tumor. The purpose of this study is to determine the systematic and random errors using 3D surface tracking system in breast cancer. The characteristics of AlignRT system were performed and the correlation between CBCT and AlignRT was also verified. In clinical application, the 11 left side breast cancer patients who were treated with DIBH technique in TrueBeam linear accelerator were selected. The AlignRT was used for patient setup and tracking the patient's position during treatment. The real-time 3D surface image was generated by AlignRT and registered to planning CT image (CT_S) or captured image in the first session (ART_S) as the reference image. Where the patient position deviated from reference image in vertical, longitudinal and lateral directions were recorded. Then the systematic and random errors were calculated. The characteristics of the AlignRT system with new version of 3 camera pods showed no effect to the infrared light in some factors such as gantry angle and usage time, however, there were some factors having a small effect on the infrared light, those are room light intensity level, skin tone protocol, region of interest and couch angle. These effects may influence the creation of a real time 3D surface image and also impact on the detection of displacement error by AlignRT system. In correlation between AlignRT and CBCT, the results yielded very good agreement each other and also excellent agreement with known couch shifting that implied AlignRT is the high accuracy system and can detect the displacement error with the same efficiency as the CBCT system. For the clinical application, the intrafraction motion error from patient setup uncertainty is about half of interfraction motion error, which is less impact due to the stability in organ movement from DIBH. The systematic reproducibility also has half of random error because of the high efficiency of modern linac machine that can reduce the systematic uncertainty effectively, while the random error is uncontrollable. The average systematic error for all directions in both LMT and LLT fields was 0.47 ± 0.03 mm, while the average random error was 1.25 ± 0.08 mm. It can be concluded that the AlignRT system could be used to determine the patient setup variation in fractionate radiotherapy for left breast cancer patients when using DIBH technique in sub-millimetre level.

KEY WORDS: 3D SURFACE TRACKING SYSTEM / SYSTEMATIC AND RANDOM ERRORS / INTER AND INTRAFRACTION / ALIGNRT/ DIBH

97 pages

การหาความคลาดเคลื่อนแบบระบบและแบบสุ่ม จากการใช้ระบบภาพ 3 มิติตรวจจับตำแหน่งแบบตลอดเวลาในผู้ป่วยมะเร็งเต้านม

THE SYSTEMATIC AND RANDOM ERRORS DETERMINATION USING REAL-TIME 3D SURFACE TRACKING SYSTEM IN BREAST CANCER

จารึก ก้านเพชร 5637832 RAMP/M

วท.ม. (ฟิสิกส์การแพทย์)

คณะกรรมการที่ปรึกษาวิทยานิพนธ์: นवलเพ็ญ คำรงกิจอุดม, Ph.D., ทวีป แสงแห่งธรรม, Ph.D.

บทคัดย่อ

เทคโนโลยีและเทคนิคในการรักษาโรคมะเร็งได้มีการพัฒนาก้าวหน้าไปอย่างมาก มีการนำระบบภาพนำวิถี (IGRT) มาใช้เพื่อตรวจสอบตำแหน่งของการฉายรังสีก่อนการรักษาทำให้สามารถลดปริมาณรังสีและผลข้างเคียงของเนื้อเยื่อที่อยู่รอบๆก้อนมะเร็ง ในขณะที่เดียวกันยังสามารถเพิ่มปริมาณรังสีที่ก้อนมะเร็งได้ วัตถุประสงค์การศึกษาเพื่อต้องการหาค่าความคลาดเคลื่อนทั้งแบบระบบและแบบสุ่มในผู้ป่วยมะเร็งเต้านมที่ได้รับการรักษาด้วยรังสีโดยใช้เทคนิคการหายใจเข้าและกลืนใจ (DIBH) ขณะฉายรังสีโดยใช้ระบบภาพสามมิติแบบตรวจจับตลอดเวลา มีการศึกษาคุณลักษณะของระบบ AlignRT และหาความสัมพันธ์ระหว่างค่าความคลาดเคลื่อนจาก CBCT และระบบ AlignRT ในการประยุกต์ใช้ทางคลินิก ทำการศึกษาในผู้ป่วยจำนวน 11 ราย ที่ได้รับการฉายรังสีในห้อง TrueBeam และใช้อุปกรณ์ตรวจจับตำแหน่งของการฉายรังสีโดยระบบภาพสามมิติแบบตรวจจับตลอดเวลาทั้งก่อนและขณะฉายรังสี หาค่าความคลาดเคลื่อนของตำแหน่งการฉายรังสีในแนว หน้า-หลัง บนล่าง และซ้าย-ขวา เพื่อนำไปคำนวณหาค่าความคลาดเคลื่อนแบบระบบและแบบสุ่มที่เกิดขึ้น จากคุณลักษณะของระบบสร้างภาพสามมิติแบบตรวจจับตลอดเวลาที่มี 3 ชุดกล้อง พบว่า สามารถลดผลกระทบจากบางปัจจัยที่มีต่ออินฟราเรด เช่น มุมของการหมุนแกนทรีและระยะเวลาการใช้งาน มีบางปัจจัยที่มีผลต่อความคลาดเคลื่อนเล็กน้อยจากการสร้างภาพ เช่น ระดับแสงในห้องฉายรังสี การเลือกโปรโตคอลที่เหมาะสมกับสีผิวผู้ป่วย การเลือกบริเวณพื้นที่ที่สนใจและมุมการหมุนเตียง ผลความสัมพันธ์ของความคลาดเคลื่อนที่ได้จากระบบ AlignRT และ CBCT พบว่า ระบบทั้งสองให้ค่าความคลาดเคลื่อนที่สอดคล้องกันอย่างดีและตรงกับค่าการเลื่อนเตียงที่แท้จริง ในส่วนผลของทางคลินิก พบว่าความคลาดเคลื่อนที่เกิดจากการการขยับตัวของผู้ป่วยระหว่างการฉายรังสีมีผลประมาณครึ่งหนึ่งของความคลาดเคลื่อนในการจัดทำผู้ป่วยในแต่ละครั้ง เนื่องจากการใช้เทคนิคการหายใจเข้าสูดและกลืนใจ ลดการเคลื่อนที่ของอวัยวะระหว่างการฉายรังสี ค่าเฉลี่ยความคลาดเคลื่อนแบบระบบอยู่ที่ 0.47 ± 0.03 มม. ขณะที่ความคลาดเคลื่อนแบบสุ่มมีค่าเฉลี่ยอยู่ที่ 1.25 ± 0.08 มม. ค่าความคลาดเคลื่อนแบบระบบมีค่าน้อยกว่า เนื่องจากประสิทธิภาพของเครื่องฉายรังสีรุ่นใหม่ที่มีทันสมัย ทำให้สามารถลดค่าความคลาดเคลื่อนแบบระบบได้อย่างมีประสิทธิภาพ ในขณะที่ค่าความคลาดเคลื่อนแบบสุ่มนั้นยังไม่สามารถควบคุมได้

CONTENTS

	Page
ACKNOWLEDGEMENTS	iii
ABSTRACT (ENGLISH)	iv
ABSTRACT (THAI)	v
LIST OF TABLES	vii
LIST OF FIGURES	ix
LIST OF ABBREVIATION	xi
CHAPTER I INTRODUCTION	1
CHAPTER II OBJECTIVE	5
CHAPTER III LITERATURES REVIEWS	6
CHAPTER IV MATERIALS AND METHODS	28
CHAPTER V RESULTS	43
CHAPTER VI DISSCUSION AND CONCLUSION	55
REFERENCES	63
APPENDICES	67
BIOGRAPHY	97

LIST OF TABLE

Table	Page
5.1 The displacement of phantom position between captured image and reference image (ART_S and CT_S) for repeatability image effect.	43
5.2 The reproducibility of camera reading of ART_S reference image.	44
5.3 The value of setup error detected by the AlignRT system during rotate gantry to full rotation used the ART_S for reference image.	45
5.4 The value of setup error detected by the AlignRT system during rotate gantry to full rotation used the CT_S as a reference image.	46
5.5 The phantom position error detected by AlignRT comparing with ART_S and CT_S reference image on room light condition.	47
5.6 The setup error detected to rando phantom (black surface) by the AlignRT system used ART_S and CT_S for reference image.	47
5.7 The setup error detected to surface phantom of AlignRT (white surface) by the AlignRT system used ART_S reference image.	48
5.8 The detected shifted of the rando phantom on different region of interest selection.	48
5.9 The setup error detected every 10 degree by the AlignRT system during rotate couch angle from 270 to 90 degree compared with both the ART_S and CT_s for reference image.	49
5.10 The displacement error detected by the AlignRT on time effect compared with the ART_S reference image.	50
5.11 Couch position value between known couch and actual position.	51
5.12 The displacement errors in three major directions detected by the AlignRT system and with the automatic matching software of CBCT compared with known couch shifted.	52

LIST OF TABLE (cont.)

Table		Page
5.13	The correlation factor calculated from Pearson correlation formula to illustrate relationship among the AlignRT system and the CBCT system and known couch shift values.	53
5.14	The population systematic and random error from inter-and intrafraction of LMT and LLT field.	54
5.15	The systematic and random errors combined effect of inter- and intrafraction motion in one index.	54

LIST OF FIGURES

Figure	Page
3.1 The mammography of (a) normal breast and (b) breast with cancer (white arrow).	7
3.2 The mammography of (a) normal breast and (b) breast with cancer (white arrow).	7
3.3 The patient during treated with chemotherapy The beam free path	8
3.4 The beam free path from lateral tangential field during (a) free breath and (b) deep inspiration breathe hold.	10
3.5 The AlignRT report shown the treatment can start while all the real-time deltas are still within tolerances	11
3.6 The diagram of 3D photogrammetry process measured from two photographic images obtained from different positions	11
3.7 The camera pod of the AlignRT system	12
3.8 The AlignRT system installed with TrueBeam linear accelerator	13
3.9 The reference image that (a) generated in the first treatment session by extraction of the surface image from CT data (ART_S) and used (b) the planning CT surface contours (CT_S)	14
3.10 The overall process of radiotherapy treatment.	15
3.11 Set-up error in Patient 1 (mm)	23
3.12 Set-up error in Patient 2 (mm)	23
3.13 The impact of geometric deviations	24
4.1 Linear Accelerator: TrueBeam with 3D on-board CT and 3D surface tracking.	28
4.2 Computed tomography simulator.	29

LIST OF FIGURED (cont.)

Figure	Page
4.3 Anderson rando phantom	30
4.4 The camera pod of AlignRT	32
4.5 Surface phantom of AlignRT	32
4.6 Calibrate plate	33
4.7 Light meter	33
4.8 The setting up of calibrate plate for monthly QA check	34
4.9 The surface phantom of AlignRT on treatment couch	35
4.10 The rando phantom setting up in dark room light condition	36
4.11 ROI condition for region of interest effect.	37
4.12 The rando phantom setting up for Couch angle effect study. (a) 270 degree couch angle. (b)	38
4.13 The set up condition for correlation between AlingRT and CBCT.	40
4.14 Report of AlignRT.	42
6.1 The displacement errors during rotate the gantry between 3D surface image and ART_S surface image.	56
6.2 The displacement errors during rotate the gantry between 3D surface image and CT_S surface image.	57
6.3 The graph of displacement error on various couch angle compared with ART_S reference image in vertical, longitudinal and lateral directions.	58
6.4 The graph of displacement error on various couch angle compared with CT_S reference image in vertical, longitudinal and lateral directions.	59

LIST OF ABBREVIATIONS

Abbreviation	Term
2D	Two dimensional
3D-CRT	Three dimensional conformal radiation therapy
AAPM	American Association of Physics in Medicine
ART_S	Previous captured of AlignRT reference image
CBCT	Cone beam computed tomography
CT	Computed tomography
CT_S	Planning CT reference image
EPID	Electronic portal imaging device
IGRT	Image guided radiation therapy
IMRT	Intensity modulated radiation therapy
kV	Kilo voltage
LINAC	Linear Accelerator
OBI	On board imager
OAR	Organ at risk
SD	Standard deviation
TPS	Treatment Planning system
VMAT	Volumetric modulated arc therapy

CHAPTER I

INTRODUCTION

Radiotherapy is one of the important modalities for cancer treatment that can be used to treat patient both curative and palliative method. The aim of treatment is to deliver a high dose to tumor while reserving normal tissue to by minimizing dose for curative radiotherapy and acquire the better quality of life to patient for palliative radiotherapy[1, 2]. It may be cooperated with other modalities such as surgery and chemotherapy. However, radiation therapy treatment is a local treatment because only the cells in treatment field or adjuvant area are affected then it cannot cure cancer that has already spread to a part of body. In another way, the radiotherapy must have the high accuracy and precision to deliver radiation into the target with least effect for normal tissue.

Several modality imaging are used for radiotherapy planning to determine tumor and organ at risk (OAR) and for designation of the appropriate beam direction. At present, the 3D images included Computed Tomography (CT), Magnetic Resonance Imaging (MRI) or Positron Emission Tomography (PET) are commonly used to present the patient image and data during radiotherapy treatment process. The new treatment techniques included 3D Conformal Radiotherapy (3DCRT), Intensity Modulated Radiotherapy (IMRT) and Volumetric Modulated Arc Radiotherapy (VMAT) are developed to hit the goals of treatment result is improving radiation dose accuracy and avoid radiation effect to normal tissues.

Breast cancer is one of the most cancer incidences in Thailand and the number of people suffering from breast cancer have increased in each year[3]. The assorted treatments are used to treat breast cancer such as surgery, chemotherapy and radiotherapy. The surgery treatment way can be selected in case of local treatment that the result is quite more efficiency. The chemotherapy is utilized to treat cancer by injecting chemical medicine that will transport via blood way. This treatment method is able to affect for patient's whole body such as loss hair, skin burn or anorexia. The

radiotherapy is the most favorite treatment way for breast cancer treatment, it is the effective treatment method with local side effect. The radiotherapy procedure is divided into 3 steps.

The first, step patient is simulated by CT-simulator machine to collect patient data. The cross sectional patient images are reconstructed for other planes and then images and patient information are transferred to treatment planning system. The suitable immobilizations are chosen for individual case to make sure that patient's position is still in the same position from simulation to treatment process. The next step is a planning process, the computed tomography data (patient's body image) including tumor and OARs are delineated by radiation oncologist, then the appropriate treatment technique and other planning parameters are displayed the high radiation dose conform to the tumor and spare radiation dose to surrounding normal tissue. The last step is treatment process that the treatment plans are sent to treatment system. This process is needed to verify before radiation beam delivery to make sure for the right dose to the right site.

The various modalities of Image Guide Radiation Therapy (IGRT) can be used to verify the correct position of treatment field and check patient's position to be the same as position at simulator room. The examples of IGRT are Electronic Portal Imaging Device (EPID), On-Broad Imager (OBI), Cone Beam Computed Tomography (CBCT) and AlignRT etc.

The EPID and OBI[4, 5] are used for patient's position verification by generating the orthogonal radiography images with MV beams. The images are captured 2 planes in both antero-posterior and lateral views and compare with reference images from Digitally Reconstructed Radiograph (DRR) generating from CT-simulated data. The EPID images show the lower image quality compared with OBI image due to the Compton effect on MV image. Both imaging modalities are easy and convenient to use with less time to reconstruct but they can display in only 2D view.

To solve the problem of 2D images, the CBCT[6-8] was invented to display the image in 3D view. The CBCT can be generated from kV beam that can give the high quality image with soft tissue detail. The patient setup errors are observed by comparing between the CBCT image in treatment room and reference

planning CT image from CT simulator room. Because this modality can display the patient data in both soft tissue and bone detail with 3D image, so it made CBCT in favorite modality of patient's setup error. However, CBCT technique can operate only at couch angle position at 0 degree and use ionizing radiation to generate image. Moreover, it is not real-time technique that can monitor the patient's position during treatment.

The AlignRT, 3D surface tracking system[9-11], is used to setup and verify patient's position both before and during treatment. This system was installed at King Chulalongkorn Memorial Hospital in March 2015 in treatment room (TrueBeam linear accelerator) as another image guide beside CBCT. AlignRT is the software component that a part to ensure that the corrected areas of patient's body are targeted by radiation. It is a video-based three-dimensional (3D) surface imaging system that can create the patient's surface image and can be used to determine the location of the patient instead of using the anatomical structure before and during radiotherapy treatment. The advanced software, a computer workstation and 3D camera units are consisted in the system. Because the infrared light is used instead of radiation to detect patient position, therefore this system is non-invasive and does not require the body marker to be put on patients.

In the tracking mode, AlignRT can acquire a continuously image of patient and perform as a monitoring and tracking system. The optimum treatment position during treatment simulation is first generated as a reference surface of AlignRT. This reference image is generated by either recording the surface of a patient placed in the treatment room or by importing skin contours from CT volumetric data generated via third party treatment planning software. The patient's position is acquired before each treatment and compared to the reference image by the system's surface matching software. The displacement error is detected and the software calculates the new location and displays to the right position of the patient. The software will hold the delivered beam suddenly when the patient's position uncertainty are larger than the destine threshold and can treat again if the error is under the thresholds.

The breast cancer patients are commonly treated by radiotherapy. The side effect may be occurred by exposed radiation dose to critical organ included suddenly

and long-term effect. Heart disease is one of long-term effects caused radiation dose from left breast cancer treatment to the left ventricle and left ascending coronary.

The Deep Inspiratory Breath Hold (DIBH)[12] is the technique that can be applied to avoid the side effect from breast cancer treatment, especially for left side. The patient is suggested to deep inhale and hold during deliver radiation beam. The increasing of lung volume pushes heart up that makes more distance between heart and chest wall. The received heart dose can be reduced when chest wall to lung distance increases[13-15]. However, the success of DIBH technique is occurred by the patient need to still in the same position during treatment like the same position in simulator room. The AlignRT is used to setup and monitor the breast patient's position to still in the same position during treatment with DIBH technique to avoid the long-term side effect of heart.

This AlignRT device is the first 3D surface tracking system in Thailand that is strongly needed to study the characteristics before using for the patient. Therefore, one purpose of this research is to study the characteristics of AlignRT system. There are many factors that may influence to AlignRT image reconstruction such as room light, time, gantry angle, couch angle, skin tone protocol and region of interest. After knowing about characteristics of this system, the detected errors from AlignRT are compared with CBCT, the routine IGRT used current in our clinic. Then, AlignRT is applied to clinical case for breast treatment with DIBH technique to verify the patient setup error before treatment as inter fraction motion and patient movement during treatment as intrafraction motion in terms of systematic and random principle.

CHAPTER II

OBJECTIVES

The objectives of this study were:

1. To study the characteristics of the AlignRT system as a 3D surface tracking system.
2. To determine the systematic and random errors using the real-time 3D surface tracking system of breast cancer treatment with DIBH technique.

CHAPTER III

LITERATURE REVIEWS

3.1 Overview

3.1.1 Breast cancer

Breast cancer is a disease in which malignant cells developed from breast tissue. Breast cancer is the common cancer in Thai women, the second to cervical cancer, that mostly occurs in women age 40 and older and is more common in women with no children and having children late. The statistics from the National Statistics Institute showed that Annual fatalities during 2006-2013 are the leading cause of cancer death in Thailand and mortality rate has been increasing from 52,062 cases in year of 2006 to 67,694 cases in 2013. Data from the National Cancer Institute found that the increasing of incidence was by 20.5 per 100,000 population in 2007 to 26.4 per 100,000 people in 2013[3]. The risk factors for developing breast cancer are female sex, obesity, lack of physical exercise, drinking alcohol, hormone replacement therapy during menopause, ionizing radiation, early age at first menstruation, having children late or not at all, and older age[16]. Breast cancer is commonly developed from cells lining of milk ducts and lobules that supply the ducts with milk. The cancer that developed from the ducts call ductal carcinomas, while that developing from lobules is known as lobular carcinomas. The diagnosis of breast cancer is confirmed by taking a biopsy of the concerning lump. Once the diagnosis is made, further tests are done to determine if the cancer has spread beyond the breast and which treatments it may respond to. The mammogram images that compared between normal breast and breast with cancer are displayed in figure 3.1.

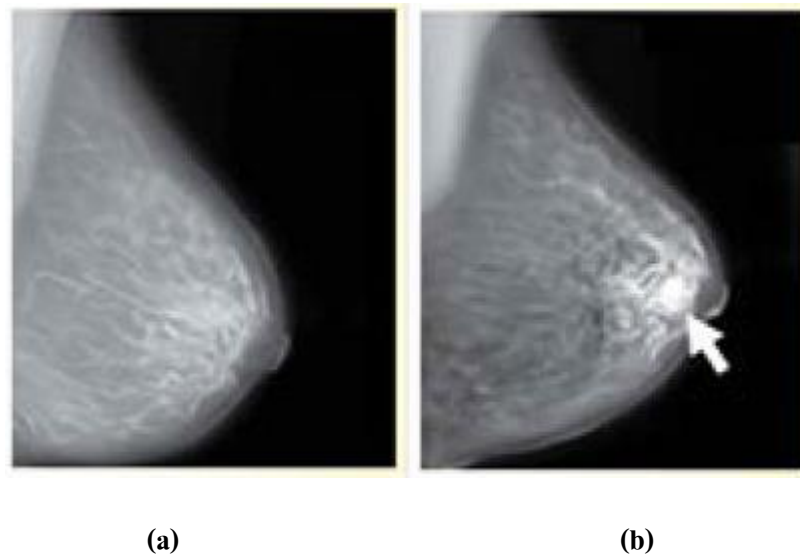


Figure 3.1 The mammography of (a) normal breast and (b) breast with cancer (white arrow).

3.1.1.1 Treatment

Breast cancer treatment depends on several factors such as type of cancer, cancer staging, hormones responding, and cancer gene. The most common methods to treat breast cancer are surgery, chemotherapy and radiotherapy.

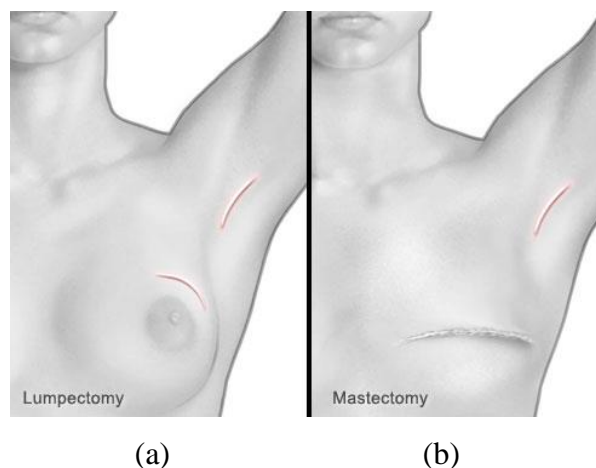


Figure 3.2 Breast surgery methods (a) breast conserving surgery and (b) mastectomy

The breast surgery method is divide to 2 ways that is breast conserving surgery and mastectomy[17] as shown in figure 3.2. Breast conserving surgery is the surgery to remove the cancer, rounding breast tissue and lymph node

called “lumpectomy” while surgery to remove the cancer, rounding breast tissue, lymph node and some muscle under breast tissue is call “segmental lumpectomy”. In the common ways after the lumpectomy surgery finished, radiation therapy is often required but it is not recommended for some patients group include the patient who had received chest radiation before surgery is over 70 year old, has cancer size less than 2 cm and can be removed cancer completely, etc. Another ways of the breast surgery method is mastectomy that surgery to remove the breast tissues, lymph nodes in the armpit and the muscle under breast tissues. Which has a variety of mastectomy surgical procedures such as “simple mastectomy” is surgery to remove a breast tissues but not for lymph nodes and muscle, “modified radical mastectomy” is surgery to remove the breast tissues, lymph nodes and some muscles under breast tissues and radical mastectomy is surgery to remove the whole breast, all axillary lymph nodes and the muscles under breast out.



Figure 3.3 The patient during treated with chemotherapy.

Chemotherapy is predominantly used for cases of breast cancer in stages II to IV, and is particularly beneficial in estrogen receptor-negative disease. The chemotherapy medications are administered in combinations with others modalities, usually for periods of 3–6 months. Most chemotherapy medications work by destroying fast-growing and/or fast-replicating cancer cells, either by causing DNA damage upon replication or by other mechanisms. However, the medications also damage fast-growing normal cells, which may cause serious side effects. The figure 3.3 shows the patient during chemotherapy treatment.

Radiation therapy is an important role in treating all stages of breast cancer because it is so effective and relatively safe. It may be appropriate for patient with stage 0 through stage III breast cancer after lumpectomy or mastectomy. Radiation can also be very helpful to people with stage IV cancer that has spread to other parts of the body. Radiation therapy can be delivered as external beam radiotherapy, the most common type, usually starts about 3 to 6 weeks after surgery or as brachytherapy is given in the operating room during surgery, just after the cancer tissue has been removed but before the opening in the skin has been closed. Radiation technique that gives radiation at the time of operation on the breast cancer is called, intraoperative. Radiation can reduce the risk of recurrence by 50–66% ($1/2 - 2/3$ reduction of risk) when delivered in the correct dose[18] and is considered essential when breast cancer is treated by removing only the lump.

3.1.2 Basic principle of DIBH technique [12-15]

Deep inspiration breast hold (DIBH) is the cardiac sparing technique to treat left side breast cancer. By supervising a patient holding breathe at deep inspiration level for both planning CT scan and a time during radiotherapy treatment. Then deliver tangent radiation beams to effectively treat cancer while reducing the dose to the heart because the action of holding breath inflates the lungs and pushes the heart away from chest wall and away from the area being treated. This technique is important to minimize potential radiation damage to the heart as shown in figure 3.4 with DIBH technique for the left breast treated because heart sits behind the left breast and chest wall.

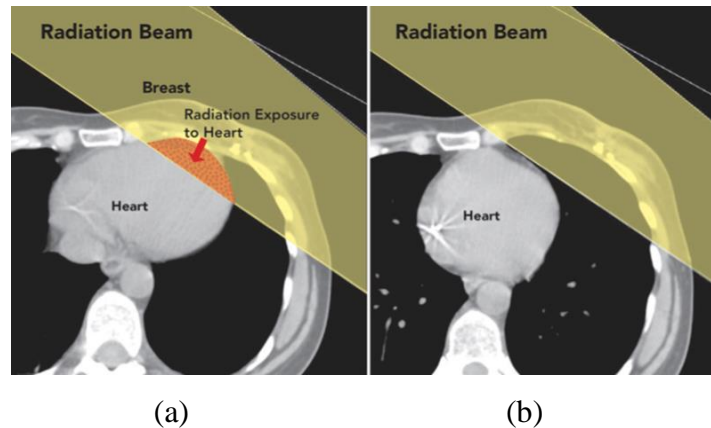


Figure 3.4 The beam free path from lateral tangential field during (a) free breath and (b) deep inspiration breath hold

The patients who were treated with DIBH would be performed with breath hold CT scan. The skin rendering of the breath hold CT is generated and transferred to the AlignRT beam hold system. Region of interest (ROI) of reference CT image is selected for matching to CBCT image during the treatment. There are two criterions for the ROI selection. First, the ROI needs to cover the treatment area. Second, it is important to include some computer vision distinguishable features to assure the accuracy of the surface matching result. As everyone is different due to patient's size, shape and internal anatomy then the patient should be performed the first planning CT scan before considering of DIBH. For some patient, even when breathing normally, the heart is not being in the radiation field, so for these case the DIBH are not necessary.

On the treatment day, the patient is first setup based on the conventional tattoos and laser system. Then, the patient is trained the breathing and is guided to take a deep breath and hold by technologist. The AlignRT Beam Hold system obtains real-time patient surface images and registers it to the reference image. The registration result displays in the six degrees (vertical, longitudinal, and lateral, rotational, roll and pitch) displacements and the magnitude of displacement. The magnitude of displacement is the Euclidian norm of the three translational displacements. All six displacements are called real-time deltas. While the patient is still holding breath, the patient will be instructed to breathe for within pre-selected tolerances. If all the real-time deltas are still within tolerances, the treatment can start as shown in figure 3.5.

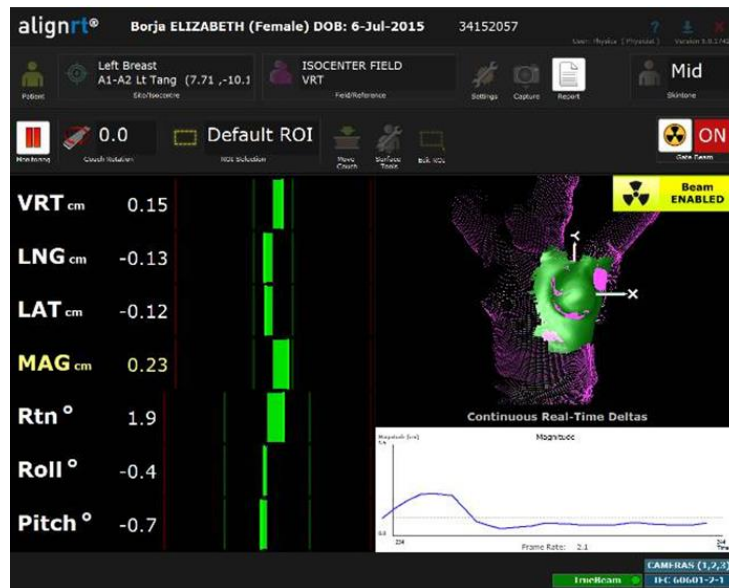


Figure 3.5 The AlignRT report with the real-time deltas and tolerances limits.

3.1.3 The surface mapping technology[9, 11, 19]

Basic Principle

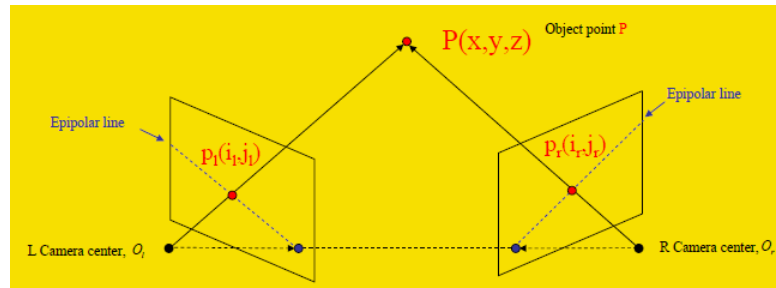


Figure 3.6 The diagram of 3D photogrammetry process measured from two photographic images obtained from different positions.

The photogrammetry, literally translated as “light-drawing measurement” is defined as the process through which geometric properties of a particular object are determined from a photographic image. In its rudimentary form, one can calculate the distance between two points lying on a plane parallel to the plane of the photographic image using a photograph’s known scale. For more sophisticated technique, or stereophotogrammetry, permit the estimation of the 3D coordinate of a point on an object through measurements made between two or more photographic images

obtained from different positions as shown in figure 3.6. As common point of particular object are identified on each photographic image, rays representing the camera's line of sight to a particular point are constructed. The intersection of several rays permits the triangulation of the point into three dimensions. With the assistance of robust computer algorithms, this simple process calculates the coordinates of several thousand points and serves a practical technique in IGRT.



Figure 3.7 The camera pod of the AlignRT system

The two or three camera pods are suspended from the ceiling of the treatment room. Each pod is equipped with a stereovision camera (two charge-coupled device cameras separated by a known baseline), a texture camera, a clear flash, a flash for speckle projection, and a slide projector for speckle projection as shown in figure 3.7. The “Speckle” refers to an optically projected pseudorandom gray scale pattern to enable the 3D reconstruction of a surface. Each pod acquires 3D surface data over approximately 120° in the axial plane, from midline to posterior flank. On the basis of a proprietary calibration process, the data are merged to form a single 3D surface image of the patient. In the overlap region near the midline, the surface from the two pods merge smoothly with less than a 1 mm root mean square (RMS) discontinuity. A daily calibration verification procedure, easily performed during the linac warm-up period, is recommended by most vendors to check the consistency of the overlap region.

The AlignRT systems include proprietary software designed to facilitate patient setup, achieved by acquiring an image of the patient and aligning this new surface with a known reference topogram. Depending on clinical workflow, a

topogram can be obtained prior to the first treatment session with the patient on the linac couch, at the time of patient simulation if a second imaging system is installed in this location, or by the extraction of the patient's external surface contour at the time of virtual simulation with the contour transferred via digital imaging and communications in medicine (DICOM) to the AlignRT system. An alignment tool allows for the comparison of the topogram with the newly acquired images. During patient alignment, the software calculates the optimal couch translation and rotation to bring a newly obtained topogram into congruence with a clinician-defined region of interest on the topogram. Any extraneous surfaces irrelevant to patient alignment should be removed to ensure the accuracy in treatment field position. The entire process takes less than 10 seconds, and can be repeated to satisfy institutional localization standards.



Figure 3.8 The AlignRT system installed in TrueBeam linear accelerator

The AlignRT system (VisionRT, Ltd., London, UK) is a commercial solution that uses surface alignment technology[9]. The 3D surface image is created by using the AlignRT software and captured using the 3D cameras as shown in figure 3.8, which projected a bright speckle pattern across the patient for several seconds. The acquired 3D surface image is generated and compared with the reference image that can be obtained at the first treatment session by extraction of the surface image from CT data (ART_S) or used the planning CT surface contours (CT_S) are shown in figure 3.9.

The system software is used to produce three planar translations required for precise reproduction of the patient's expected position. All orthogonal shifts were applied to the patient, and a second image acquisition and analysis using AlignRT is performed for verification.

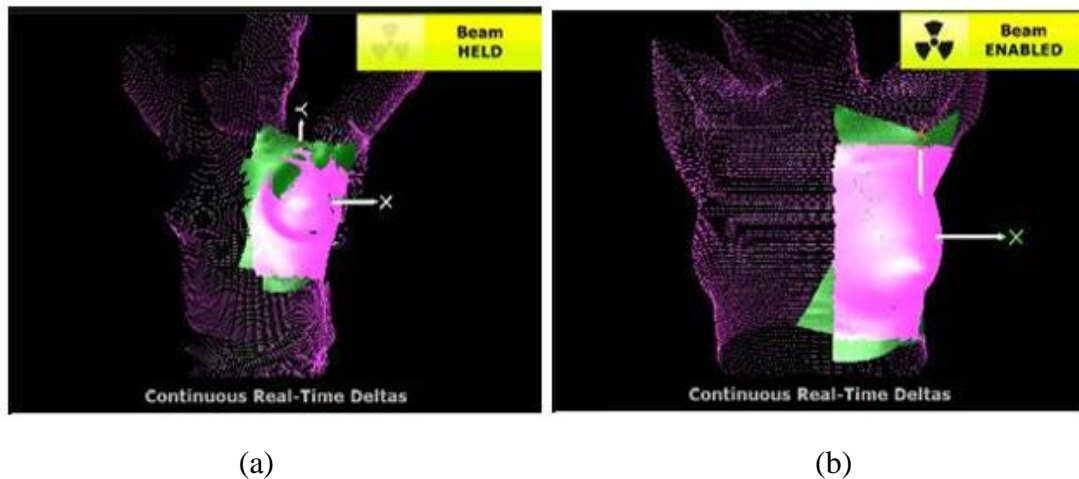


Figure 3.9 The reference image that (a) generated in the first treatment session by extraction of the surface image from CT data (ART_S) and used (b) the planning CT surface contours (CT_S)

The process generally takes less than 3 minutes, and is repeated if necessary until the suggested shifts fall below 5 mm in any plane. The AlignRT software will also calculate the volume of tissue within a specified distance from the reference image and localize regions of breast that deviate beyond the threshold.

The AlignRT system offers specific benefits for the development of IGRT programs including: (1) noninvasive; (2) rapidly data acquired, either for frequent verification of the patient localization or intrafraction patient monitoring; (3) straightforward to use for radiation therapy technicians; and (4) the ability to monitor and compare treatment progress with respect to prior sessions[20-23].

3.1.4 Work flow in advanced radiotherapy[24]

The “chain of radiotherapy” is shown in figure 3.10 for the physical and technical basis of radiotherapy that covers different aspects of all links.

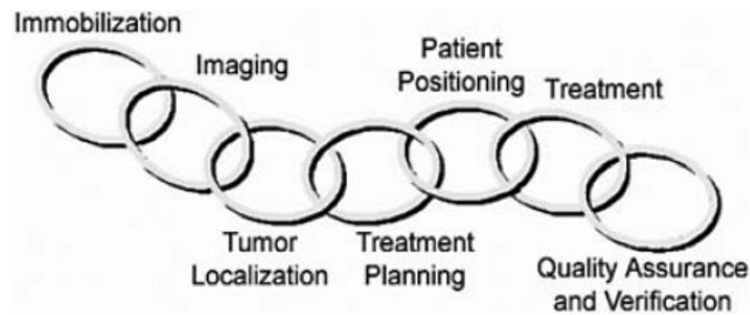


Figure 3.10 The overall process of radiotherapy treatment.

3.1.4.1 Patient immobilization

For the advanced radiotherapy, “immobilization” or the fixation of irradiated body area and organ is necessary to improve reproducibility and precision because modifications of patient’s position relative to the treatment machine can lead to dangerous of dose errors. The various immobilization devices and techniques have been applied for radiotherapy. The two fundamental rules of immobilization devices are to immobilize patients during treatment and to provide a reliable means of reproducing the patient’s position for simulation to treatment and on the other hand from one treatment to others.

3.1.4.2 Imaging and tumor localization

The multiple modalities of 3D image data set such as computed tomography (CT), magnetic resonance imaging (MRI) are the way to determine the PTV and OAR. Routinely, CT is the most common tomographic imaging method to use in this issue. These images can be registered to other modalities to define the target volume and organs at risk. The computer software, three dimensional image registrations is able to match the 3D spatial information of the different imaging modalities by using of either external or internal anatomic landmarks.

3.1.4.3 Treatment planning

The 3D treatment planning is required for the basically advanced radiotherapy. After delineating the therapy relevant structures, various therapy concepts are simulated as part of an iterative process. The search for “optimum” geometrical irradiation parameters, the “irradiation configuration” is very complex. The suitable beam directions and the respective field shapes must be

selected. The various possibilities of volume visualization, such as Beam's Eye View, Observers View, or Spherical View, are tools, which support the radiotherapist with the process.

For dose calculation step, the quality of treatment planning depends naturally on the accuracy of the dose calculation. An error in the dose calculation corresponds to an incorrect adjustment of the dose distribution to the target volume and the organs at risk. The calculation of dose distributions is the implementation of an algorithm which is fast enough to fulfill the requirements of daily clinical use, and which has sufficient accuracy. Most treatment planning systems work with so-called pencil-beam algorithms, which are semi-empiric and meet the requirements in speed and accuracy. If too much heterogeneity, such as air cavities, lung tissues, or bony structures, is close to the target volume, the use of complex algorithm such as AAA, Acuros or Monte Carlo calculations are preferred. Monte Carlo calculation is a high-end algorithm that simulates the physical rules of interaction of radiation with matter in a realistic way. In the case of heterogeneous tissue they are much more precise, but also much slower in calculation process, than pencil-beam algorithms.

After finishing the calculation step, the plans with 3D dose distribution are needed to evaluate in an appropriate way. The hot and cold spots were concerned and adjusted for better homogeneity and conformity of the dose distribution. The computer graphic and mathematical devices are developed to support the evaluation of dose distribution. The goal of treatment planning is to determinate the suitable and practicable of irradiation technique which results in a conformal dose distribution thus treatment planning is a typical optimization problem. In conventional "forward planning" a trial and error method is applied for interactive plan, while the new method of "inverse planning" for modulated radiotherapy is able to automatically calculate a treatment technique which leads to the very good coverage of the target volume and sufficient sparing of healthy tissue. At present time, the most modern and advanced technique in radiotherapy is VMAT that more advanced from IMRT. The gantry is rotated around the patient during radiation delivered with beam modulation from MLC movement, dose rate variation and gantry speed. Dose distributions can be conformed to the planning treatment volume, reduce dose to surrounding tissues and

decrease duration time of the treatment delivery. This new technology also offers the radiation oncologist for more control and flexibility to deliver a carefully targeted dose so that only the tumor receives a high dose of radiation. Three- dimensional imaging technology aids in the precision of the radiation that can help the doctor to see the tumor clearly at the time of treatment.

3.1.4.4 Patient positioning

The patient position of radiotherapy in treatment room is the link between treatment planning and the irradiation, as called the patient positioning. The problem is the accurately transfer the irradiated plans to treatment room with the same patient positioning. It can be performed with a suitable immobilization device for all process starting from simulation to treatment.

3.1.4.5 Treatment

The most essential link in the chain of radiotherapy process is treatment, itself characterized by radiation delivery. Modern radiotherapy, especially when there is curative intension, is practiced as 3D conformal radiotherapy, IMRT and VMAT. Most conformal radiotherapy treatments are performed by external radiation with photons.

3.1.5 Image-guide radiation therapy

The main goal of IGRT is to manage interfraction motion to confirm the treatment field setting up before treatment; however, it can be applied as intrafraction motion to analyze the patient movement during treatment. These two types of motion patterns are possible to apply to reduce margins and optimize treatment designs. Traditional, patients are positioned according to skin marks for radiotherapy treatment and assumes that the inside of the tumor position remain unchanged during the whole treatment course. However, this simplification has been shown to be wrong for a many tumors location, especially the tumor in moveable organ: e.g. breast cancer, prostate, lung, and liver. If the target position is not verify prior to radiation, a different position of the target could result in reduced doses to the tumor and higher than planned doses to surrounding organs at risk. Decreased rates of local control and higher rates of side effects are consequences. IGRT technology accounts for motion to ensure that the target is in the same position every treatment session for improving the precision and

accuracy of the delivery treatment results. The modern linear accelerators are normally equipped with imaging device that take pictures of the treatment fields immediately to verify tumor position prior to treatment.

There are many IGRT types, that ranging from portal imaging, diagnostic x-ray imaging, in room CT (both conventional and cone-beam with kilovoltage and megavoltage) and intrafraction tumor tracking.

Portal imaging has progressed from the use of film as the imaging detector, through screen/camera imagers and liquid ionization chambers, to solid-state flat panel detectors. The EPID, flat panel detector fitted to the linear accelerator and a component that digitizes and displays the images on the computer screen, is emerging as the new standard 2D detector for portal imaging IGRT using MV beams. Recent developments include the software to analyze the portal images and compare them with treatment planning images of DRR.

Diagnostic x-ray imaging is an additional kV x-ray source/detector system perpendicular to the treatment beam axis or 2 additional gantry mounted x-ray systems with central axes intersecting with each other at the Linac's isocenter. The approach of using diagnostic x-rays for treatment set-up verification offers a three advantage: (a) image quality (a well-documented problem in MV-based imaging) is no longer an issue, especially in combination with aSi detectors, (b) patient dose is less compared to daily MV imaging and (c) the modality can be used in fluoroscopic mode during treatment.

In-room CT is the first way to visualize soft tissue in 3D view prior to treatment and defining the spatial relationship between target and organs at risk. A conventional CT scanner is placed in the treatment room, either on the same couch axis as the LINAC gantry, or on an orthogonal axis to the gantry. A single couch serves the CT scanner and the beam delivery system. The couch is first rotated into alignment with the CT scanner to acquire a pretreatment CT. The CT scanner is mounted on rails so that it, rather than the couch, moves in the axial direction relative to the patient to collect a volumetric scan.

Cone-beam CT uses either the therapy beam itself (MV-CBCT) or a gantry mounted kilovoltage source and detector (kV-CBCT). Cone-beam CT is a full CT scan of the patient on the treatment couch that acquired immediately before treating the

patient. The time of CBCT scanned and reconstructed takes in less than 2 minutes. In order to verify the patient setup accuracy, the automatically or manually registration between CBCT and planning CT images are normally used. The purpose of image registration is to determine the translation in three directions (up-down, left-right and superior-inferior). The translation of treatment couch can be done automatically or manually to the correct position.

The AlignRT system is 3D surface imaging system. This system uses images of skin surfaces of a patient in 3D to verify the patient positioning before and during radiotherapy treatment. The system consists of advanced software, a computer workstation, three 3D camera units, cables, and templates that are used for camera calibration. The system is non-invasive and, has the advantage of using infrared light instead of radiation to detect patient positions. The AlignRT can generate a reference surface by either recording the surface of a patient placed in the treatment room or by importing body contours from CT data. Before each treatment session, the patient's image at treatment position is acquired and compared to the reference image by the system's surface matching software. When the movement or displacement from the reference position is detected, the software calculates new coordinates and adjusts the treatment couch to optimal positioning.

3.1.6 Image Registration[25]

Image registration is widely used for treatment planning, organ motion studies, image-guidance and follow up. The purpose of image registration is to find the transformation (translation, rotation, deformation) that maps one scan onto another. The scans can be combined and registered on a pixel-by-pixel basis (e.g., for target volume delineation), or differences can be quantified (for image guidance and follow up). In radiotherapy, image registration is mostly used to align rigid structures e.g., bone, from reference image to other image set. Bone acts as a frame of reference for treatment relative to which the position of organs of interest is determined. In this study, the first image registration is performed using the registration between CT planning and the CBCT before treatment to check the patient set up error. After that the patient is moved to the correct position before treat the patient.

3.1.7 Type of motion[26, 27]

The motion in radiotherapy issue can be divided into 2 categories.

3.1.7.1 Interfraction motion

The patient position changes between treatment sessions, i.e., patient setup changes and patient anatomy changes (tumor shrinking, organ fill status).

3.1.7.2 Intrafraction motion

The patient position changes during a treatment session, i.e., breathing, gas passing and uncooperative patient.

Both of these motions may affect to systematic and random errors.

3.1.8 The set-up error definitions

The term of “set-up error” describes the discrepancy between intended and actual treatment position. It comprises of systematic and random components.

It is normally calculated as a shifted in treatment field position when a treatment image is compared against its corresponding reference. The set-up error may be determined relative to the isocenter, the field borders or both and can contain translational and rotational information.

3.1.8.1 Systematic error (Σ)

The systematic component of any error is a deviation that occurs in the same direction and similar magnitude for each fraction throughout the treatment course. The systematic error represents the mean irradiation geometry in the fractionated treatment different from the geometry in the treatment plan. The term systematic error refers to the individual patient or to the treatment population. This distribution is to be clarified as

Individual-systematic error for individual patient is the mean error over the course of treatment.

Population-systematic error for a group of patients is an indication of the spread of individual mean error. It is calculated as the standard deviation (SD) of the distribution of mean error from each individual patient and it is given in the capital sigma symbol (Σ).

Systematic errors may be introduced into a patient's treatment at the localization, planning or treatment delivery phases. For this reason, these types of errors are often referred to treatment preparation errors. Systematic error will occur in each treatment fraction. Possible treatment preparation errors are summarized below.

Target delineation error may be introduced when the CTV is first delineated and represented the difference between the defined and ideal CTV.

Target position and shape – this is a change in target position and shape between delineation and treatment. Possible causes include tumor regression or growth, bladder filling and rectal distension.

Transfer error – this is the error that accumulates when transferring image data from initial localization through the treatment planning system to the linear accelerator. It is measured using a test phantom and may be sub divided into geometric imaging, treatment planning system and linac geometry error. Possible causes include differences in laser alignment between CT and linear accelerator, CT couch longitudinal position indication image resolution, margin growing algorithm, field edge and multileaf collimator (MLC) leaf position, isocenter source to surface distance indication, gantry and collimator angle accuracy.

Patient setup error – this describes all cause of treatment setup error or by the phantom transfer error and includes all the errors listed under gross error. Possible causes include changes in the patient's position, shape or size i.e. weight change. It also encompasses more subtle effects such as the displacement of target relative to skin setup marks caused by the CT scan and treatment is performed on different couches. Patient setup error is only one possible component of the overall measured systematic setup error. The chosen method of treatment verification will determine how many of the above sources of systematic error will be incorporated into the measured setup error.

3.1.8.2 Random error (σ)

The random error is a deviation that can vary in direction and magnitude for each delivered treatment fraction. The random variations represent the mean deviation around fraction-to-fraction variations. The term random error refers to

the individual patient or to the treatment population. This distinction is to be clarified as

Individual – random error for individual patient is the standard deviation (SD) of the measured errors the course of treatment and quantifies and spread or error.

Population – random error for a group of patients is calculated as the mean of individual random errors and is given the lower case sigma symbol (σ).

Random error occurs at the treatment delivery stage that can be often referred to treatment (or daily) execution errors. They are summarized below. Patient setup error - these are varying, unpredictable changes arising from change in a patient's position, treatment equipment or setup methodology between each delivered fraction.

Target position and shape – the change in target position and shape between fractions. This error is essentially the same as that described above for systematic errors but accounts for motion between fractions rather than from delineation to treatment.

Intrafraction error – this describes changes in the patient's position and internal anatomy arising during the delivery of single fraction, for example, due to breathing.

Random errors are influenced by the immobilization system, patient compliance and department protocols. If a new immobilization device is introduced, it is likely that the random error will be affected. The daily setup errors plotted (in millimeters) from anterior – posterior image acquired for two patients over the course of their treatment. Patient 1 exhibits a small systematic (mean) setup compared to patient 2. Patient 1 has a larger, random spread of errors than patient 2. as illustrated in figure 3.11 and 3.12.

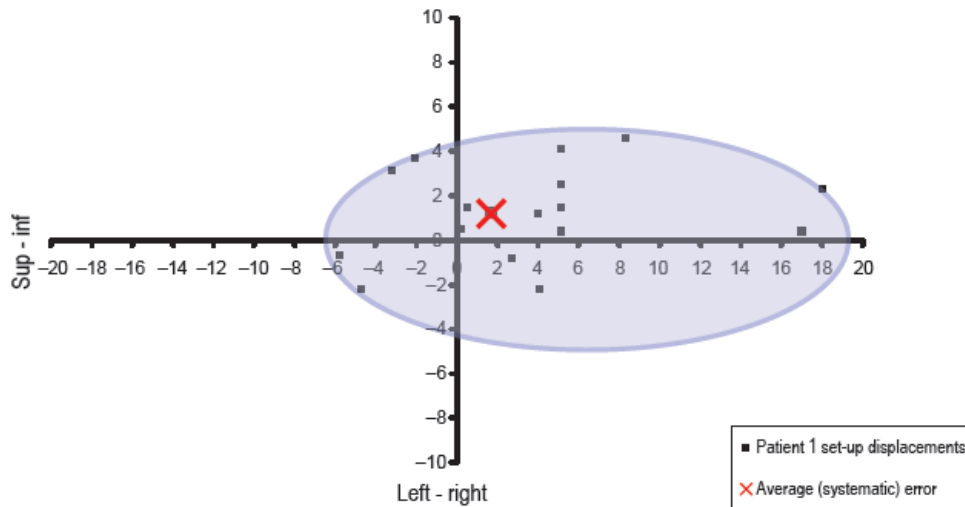


Figure 3.11 Set-up error in Patient 1

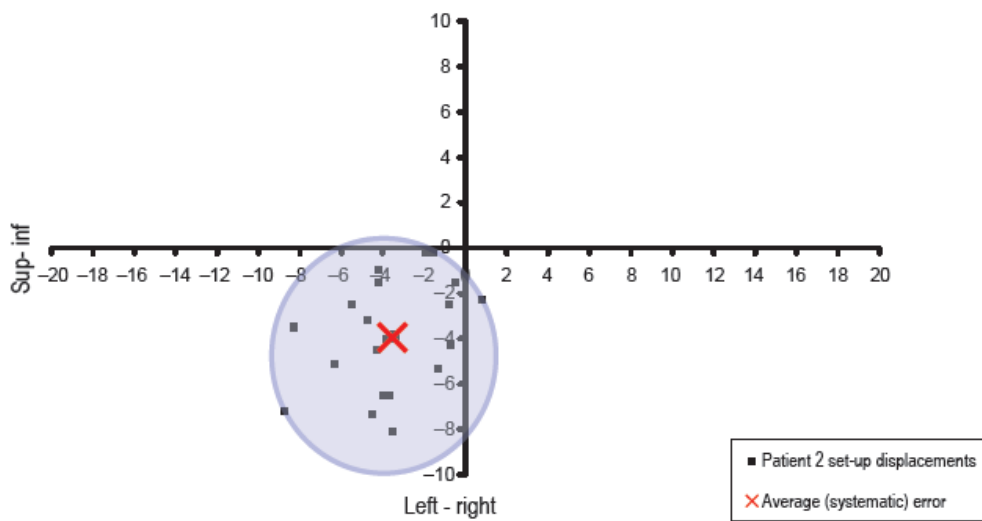


Figure 3.12 Set-up error in Patient

The considering geometric uncertainties in radiotherapy are influenced by the systematic errors, whereas random errors point in different directions for each treatment fraction. It is generally smaller value of random errors than systematic errors. The blurring effect of random errors leads to small decreasing of dose at the edge of the high dose region that will moderately affect all patients. The systematic errors, on the other hand, lead to shift the dose that will strongly affect to some patients (i.e., when the shift is such that CTV move outside the high dose

region). The impact of geometric deviations on the dose distribution is relative to the CTV. Random (Treatment execution) deviations lead to a blurring of dose distribution, while systematic (Treatment preparation) deviations lead to known shift in the cumulative dose distribution relative to the CTV as illustrated in figure 3.13 the normal situation comprise a combination of systematic and random components. The systematic error will remain throughout the course of treatment potentially compromising dose coverage to the CTV.

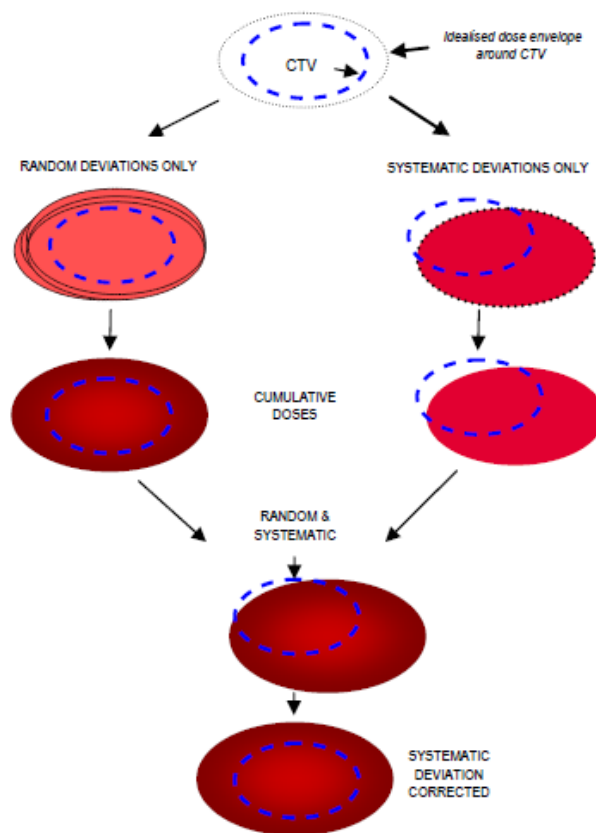


Figure 3.13 The impact of geometric deviations

3.2 Review of related Literatures

The researches related to the study of characteristic study of 3D surface tracking system (AlignRT) and the investigation of the patient's position variation of breast cancer treatment. These publish papers are presented as follows:

Letizia D et al.[28] investigated the clinical application of a technique for patient set-up verification in breast cancer radiotherapy based on a 3D surface image

registration system. The 15 breast cancer patients for conformal radiotherapy technique using the AlignRT system (VisionRT, London, UK) were performed in this study. At the initial setup, electronic portal imaging device (EPID) images were compared with Digitally Reconstructed Radiographs (DRRs) and a reference three dimensional (3D) surface image was obtained by AlignRT. Surface images were acquired prior to every subsequent setup procedure. The systematic and random errors along longitudinal and vertical directions were measured and compared for the two systems. The result showed for surface registration, the mean systematic error for AlignRT was 1.2 mm (SD = 2.8 mm) along the vertical axis and 0.7 mm (SD = 1.9 mm) along the longitudinal axis. The mean random error was 1.7 mm (SD = 0.6 mm) along the vertical axis and 1.8 mm (SD = 0.7 mm) along the longitudinal axis. The T test for systematic error showed no significant difference between measured by EPID and by AlignRT along the longitudinal ($p = 0.69$) and vertical ($p = 0.67$) axes. The T-test for random error showed a significant difference between the two systems along the vertical axis ($p = 0.05$), but not along the longitudinal axis ($p = 0.15$). These are illustrated that the AlignRT system seems to be reliable in detecting setup errors in breast cancer patients. Their results suggested that the system could be used to assess the reproducibility of patient setup in fractionated radiotherapy for breast cancer. In particular, it appears to be fast, simple and non-invasive.

Anja B et al.[29] quantified set-up uncertainties during voluntary deep inspiration breath hold (DIBH) radiotherapy using 3D-surface imaging in patients with left sided breast cancer. The 19 left side breast cancer patients were treated with radiation therapy with DIBH technique. The reproducibility of the DIBH during treatment was monitored with 2D-fluoroscopy and portal image. Simultaneously, a surface imaging system was used to capture 3D-surfaces throughout CBCT acquisition and delivery of treatment beams. Retrospectively, all captured surfaces were registered to the planning-CT surface. The interfraction and intrafraction variability were quantified in left-right, cranio-caudal and anterior-posterior directions.

For the interfraction variation, the systematic errors of translational were 0.22, 0.50 and 0.33 cm, and rotational error were 0.80° , 0.98° and 1.56° in LR, CC and AP directions, respectively. The random of translational were 0.20, 0.35 and 0.27 cm in LR, CC and AP directions, respectively, while the rotational random errors were

around 0.8° in all directions. For intrafraction rotation, the mean error was approximately zero. The mean set-up error of 0.31 cm in CC direction is potentially related to a learning curve to be able to inhale more deeply during treatment fractions compared to the deep inspiration during the planning CT-scan. Differences in deep inspiration between planning CT-scan and CBCT of up to 2.0 cm in CC direction were present during initial patient set-up.

The systematic errors were reduced to ≤ 0.14 cm; while random errors were about ~ 0.2 cm in all directions. The rotational errors did not change which was to be expected since no rotational corrections were applied.

Peng et al.[30] evaluated the localization accuracy of the AlignRT system and its tracking ability using the CBCT system and an optical tracking system. They used a Rando head-and-neck phantom with a 3 mm slice thickness CT images and five real patients, and validated the system accuracy through comparison with the CBCT system of Elekta (Elekta Oncology Systems, Norcross, GA) and the frameless SonArray optical tracking system (Zmed/Varian, Ashland, MA).

For the phantom localization study, Peng et al. used the optical tracking system to position the phantom isocenter to within 0.1 mm and 0.1° along all three axes. Their results showed that for the origin displacements, the difference between AlignRT and the CBCT systems or between AlignRT and the optical tracking systems was up to 1.3 mm and 1.7° . For phantom displacements having couch angles of 0° , i.e., if no couch rotation was needed, the difference was slightly smaller, at 0.9 mm and 0.4° for CBCT, and 0.3 mm and 0.2° for optical tracking if the references were the previously recorded AlignRT images instead of CT contour surfaces.

For large displacements of more than ± 10 mm and $\pm 3^\circ$, Peng et al. obtained a larger maximum discrepancy between AlignRT and CBCT at 3.0 mm but a smaller discrepancy of 0.4 mm between AlignRT and optical tracking. They further analyzed situation with large couch angles which we tested out in this thesis at 90° and 270° couch angles.

Peng et al. also found that the mean registration errors were smaller when using the AlignRT optical surface images than using CT contours, and for patients study, the difference in pretreatment placement was smaller between AlignRT and CBCT than between optical tracking and CBCT. Peng et al. concluded that the

AlignRT system could be used for positioning with accuracy comparable to current image/marker-based systems.

CHAPTER IV

MATERIALS AND METHODS

4.1 Materials

4.1.1 Varian TrueBeam™ linear accelerator



Figure 4.1 Linear Accelerator: TrueBeam with 3D on-board CT and 3D surface tracking system.

The Varian TrueBeam™ linear accelerator (Varian Medical System, Inc, Palo Alto, CA, USA) with the On-Board Imager (OBI) system as illustrated in figure 4.1 has photon beams of 6MV, 10MV, 6MV (FFF), 10MV (FFF) and six electron beam energies of 6, 9, 12, 15, 18 and 22 MeV. The maximum photon field size is 40x40 cm² at isocenter with the distance from the target to isocenter of 100 cm. The maximum dose rates are 600 MU/min for convention mode, 1400 MU/min for 6XFFF high intensity mode and 2400 MU/min for 10XFFF high intensity mode. The 120 Multileaf Collimator (120™ MLC) with 5 mm. leaves width for 20x20 cm² inner field and 1 cm for outer field.

The OBI is a kV imaging system that is installed on linear accelerator. The OBI presents high-quality digital images in the treatment room, allowing positioning a patient accurately before treatment. The OBI consists of a kV X-ray source and an amorphous silicon panel detector. The kV imaging system moves as the gantry rotates and shares the same isocenter to the MV treatment beam. The robotically arms can be controlled to operate three axes of motion, optimizing positioning of the imaging system. The OBI software is the program for manual or automatic registration with the Mutual information method. Both 2D radiographic projections and Cone beam computed tomography (CBCT) images could be acquired with the OBI. The CBCT uses a cone-beam x-ray source that encompasses a large volume with a single or half rotation around the patient. Image reconstructed into 3D view provides improved tumor targeting using high resolution and low-dose digital imaging. This system allows adjusting the treatment plan to anatomical changes during the treatment course of radiation therapy as called adaptive radiotherapy (ART).

4.1.2 CT Simulator



Figure 4.2 Computed tomography simulator.

The CT-Simulator scanner with 4 slices of GE LightSpeed RT (GE Medical system, Waukesha, WI, USA) illustrated in figure 4.2 is a multi-slice CT scanner with simultaneous collecting 4 rows of scanning data. The distance from tube

to isocenter is 606 mm, the distance from the tube to detector focus is 1062 mm and the bore diameter is 800 mm. The 3D images from CT were employed for treatment planning and were used as the standard for treatment field verification with CBCT.

4.1.3 Rando phantom

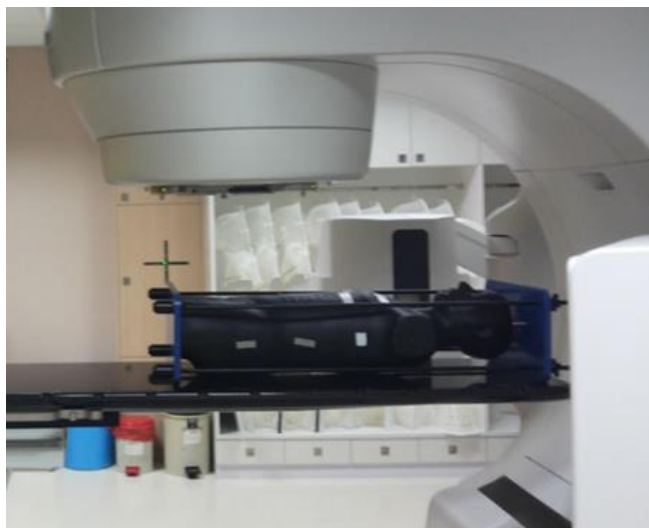


Figure 4.3 Alderson Rando phantom.

The Rando phantom (The Phantom Laboratory, Greenwich, NY, USA) incorporates materials to simulate various body tissues of human such as bone, muscle, lung and air cavities. The phantom made of tissue-equivalent material following International Commission on Radiation Units and Measurement (ICRU) Report No 44 standard with a density of 0.985 g/cm^3 and effective atomic number of 7.3. The phantom is shaped into a human torso with section into 2.5 cm transversal slices. Each slice has holes that are plugged with pin of soft tissue-equivalent, bone-equivalent or lung-equivalent. It has the option of TLD holder pin that can be inserted into the hole for measurement of dose distribution in various organs. The rando phantom is illustrated in figure 4.3.

4.1.4 Treatment Planning software

Eclipse treatment planning version 11.0.31 (Varian Medical System, Palo Alto, CA, USA) is an intergraded treatment planning system supporting radiation treatment techniques such as 2D, 3D conformal, IMRT and VMAT. There are pencil

beams, analytical anisotropic and acuros algorithms available for photon beam planning. Eclipse software is designed to increase productivity for clinicians using leading edge automated tools to contour the organs, import and optimize plans across numerous multiple linear accelerators.

4.1.5 3D surface tracking system (AlignRT)

The 3D surface tracking system, AlignRT (VisionRT Ltd, London, UK), consists of 3 camera pods, that 2 of them ceiling mounted with 30 degree angle to the treatment couch, while another pod location at the centrally foot end of treatment couch as illustrated in figure 4.4. Each camera pods is composed of 2 data cameras, white light flash and speckle projector that all pods work together to generate 3D surface image. The pods used for tracking surface of the patient with non-ionizing radiation, the pattern infrared light are projected onto surface of the patient by the projector. The dedicated software can identify pattern and generate real-time 3D surface image from the pattern infrared light with comprising approximately 20,000 points model and can be displayed within a second. The AlignRT software tracks motion of patient and compares the real-time 3D images with reference images, the captured surface image of AlignRT or the CT contour generated from treatment planning system. The AlignRT uses image registration algorithm to determine 3D transformations. The software can detect the shifted in six directions of vertical, longitudinal, lateral, yaw, pitch and rotation. When the position shifted is larger than setting tolerance for treatment, the AlignRT will hold radiation beam immediately.



Figure 4.4 The camera pod of AlignRT.

4.1.6 Surface phantom of AlignRT

The surface phantom provided by VisionRT company is the phantom simulated the human's body surface. The phantom is used to test accuracy and precision of 3D surface tracking system. The surface phantom of AlignRT is illustrated in figure 4.5.

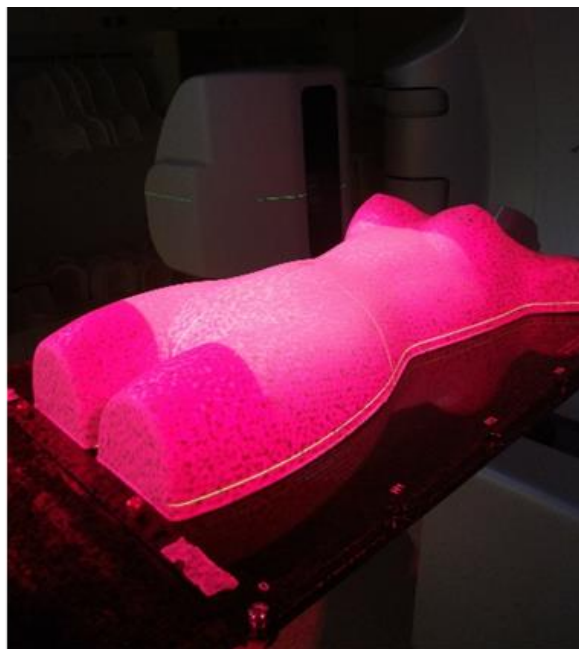


Figure 4.5 Surface phantom of AlignRT.

4.1.7 Calibration plate

The calibration plate is a white square board in size of 1.4 x 1.4 m². The plate has central cross for setting up to beam central axis, many dots and blob around 4 corner of isocenter for calibration. This plate was used to calibrate the 3 camera pods for daily and monthly camera calibration. The calibration plate is illustrated in figure 4.6.

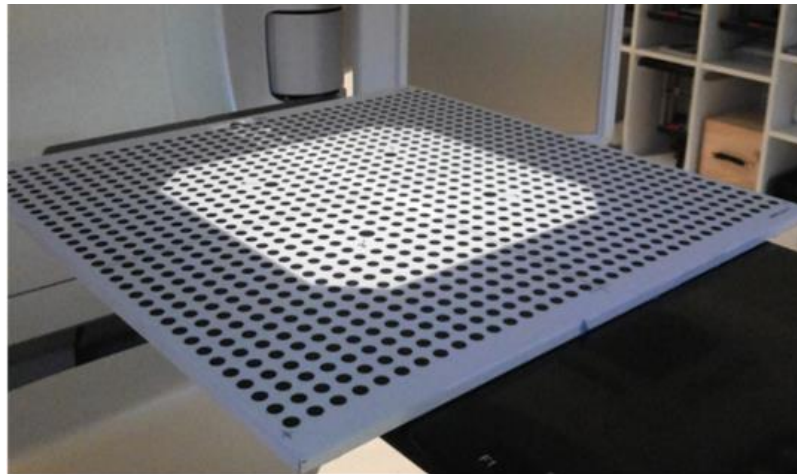


Figure 4.6 Calibration plate provided by company.

4.1.8 Light meter

The light meter (Unfors RaySafe, Sweden) is the structure for measure light level. The light meter was used for the room light effect test. The lux unit was used to define the brightness condition following the switch in treatment room. The Light meter is illustrated in figure 4.7.



Figure 4.7 Light detector and monitor.

4.2 Methods

The process was divided into 3 parts as following: the characteristics of the AlignRT system, the correlation between the AlignRT system and CBCT and the clinical application for systematic and random error data for breast cancer patients.

4.2.1 The characteristics of AlignRT

The AlignRT is the programs used for patient alignment to receive the same position with the position in CT simulator room. It is possible to improve the reproducibility of patient's position when the AlignRT was applied. The characteristics of the 3D surface tracking system should be studied before using in the clinic then the properties of AlignRT were investigated in this study.

The calibration plate was set on the treatment couch representing the patient's position as shown in figure 4.8. The monthly calibration was done before testing of the following characteristics of AlignRT system.



Figure 4.8 The setting up of calibrate plate for monthly QA check.

4.2.1.1 Repeatability of camera calibration

The surface phantom of AlignRT was set as the treatment patient's position to study the precision of AlignRT when repeating detected without new position's setup. The study was test in every 5 minutes for 10 times of

measurement. The same phantom position, bright room light condition, mid skin tone protocol and small ROI were set with only one phantom setup. The displacements of phantom position between captured image and reference image (ART_S and CT_S) results along vertical, longitudinal and lateral direction detected by AlignRT were recorded. The repeatability of camera calibration setup is illustrated in figure 4.9.

4.2.1.2 Reproducibility of camera calibration

The surface phantom of AlignRT was set representing the patient's position to study the reproducibility of AlignRT reading when camera calibration detected as shown in figure 4.9. The measurements were done everyday for 1 month. The same phantom position, bright room light condition, mid skin tone protocol and small ROI were set with repeated phantom setup. The displacements of phantom position between captured image and reference image (ART_S) results along vertical, longitudinal and lateral directions detected by AlignRT were recorded.

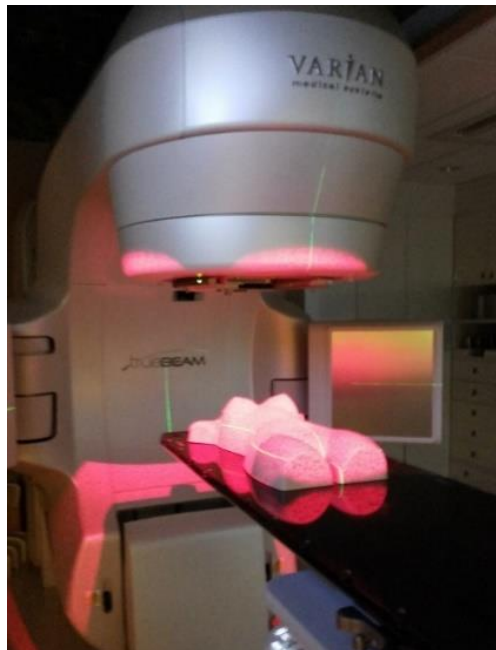


Figure 4.9 The surface phantom of AlignRT on treatment couch.

4.2.1.3 Gantry angle effect

The third camera was attached on ceiling at foot end of the treatment couch to solve problem of the blockage gantry to the camera view. This problem has an effect on the process of generating the 3D surface imaging. The gantry angle effect needed to study after new AlignRT version that the third camera was

added for testing the gantry angle dependence. The rando phantom was set on the treatment couch to the actual position. The same phantom position, bright room light condition, mid skin tone protocol and small ROI were performed. The reference image was created at zero degree gantry angle. Then, the gantry was rotated every 10 degree to the full rotation and the detected shifts by AlignRT camera between reference and real-time images in vertical, longitudinal and lateral directions were recorded

4.2.1.4 Room light effect

The room light condition that has an effect to the intensity of infrared light projected to the phantom surface may influence to the generating of 3D surface image. The phantom position was detected by AlignRT with 5 levels of the brightness conditions changing from the most brightness to the most darkness of the room light according to our room light switch as illustrate in figure 4.10. The room brightness was measured by light meter (Unfors, RaySafe, Sweden) at the location of phantom. The same phantom position, mid skin tone protocol and small ROI were acquired. The displacement of phantom position shifted in along vertical, longitudinal and lateral directions detected by AlignRT from various brightness conditions were recorded.

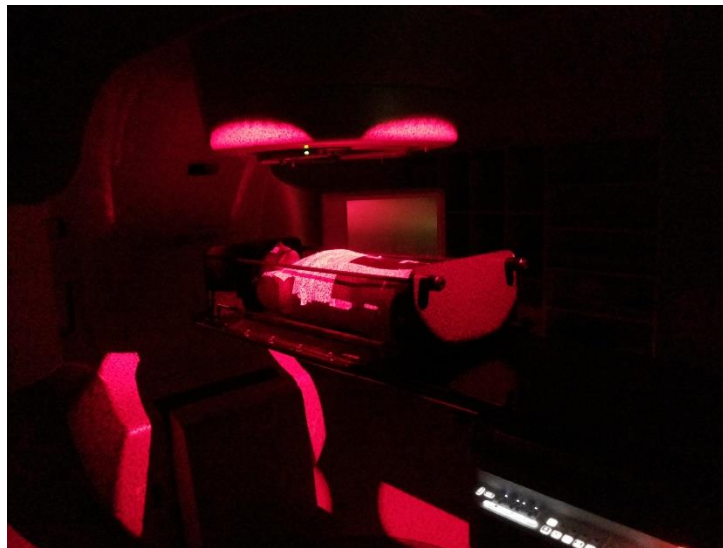


Figure 4.10 The rando phantom setting up in dark room light condition.

4.2.1.5 Skin tone protocol effect

The AlignRT has the option of fair, mid and dark skin tone protocols for matching in accordance with patient skin tone. The infrared light

intensity was different to compensate in each protocol. The 3D surface image was affected from changing in infrared light intensity. Therefore, the skin tone protocol needed to test with different skin tone of phantom. The random phantom and the surface phantom of AlignRT was represented the black and white patient skin tone. For each phantom, the 3 skin tone protocols (fair, mid and dark) were performed. The same phantom position, bright room light condition, and small ROI were set. The displacements of phantom position between captured image and reference image (ART_S) in vertical, longitudinal and lateral direction detected by AlignRT were recorded.

4.2.1.6 Region of interest effect

The various areas of ROI of 3D surface images between reference image and real-time image may result in displacement position of phantom. The size and location of these areas may influence to the generating of 3D surface image and result of imaging comparison, so the ROI effect was needed to study. The random phantom was set as the treatment patient position and position detected by AlignRT with changing of 6 ROI regions composed of small at center, cover all phantom, no ROI, cover the body at the center as default ROI, half left and half right ROIs as illustrated in figure 4.11. The same phantom position, bright room light condition and mid skin tone protocol were acquired. The displacements of the phantom position results along vertical, longitudinal and lateral direction detected by AlignRT were recorded.

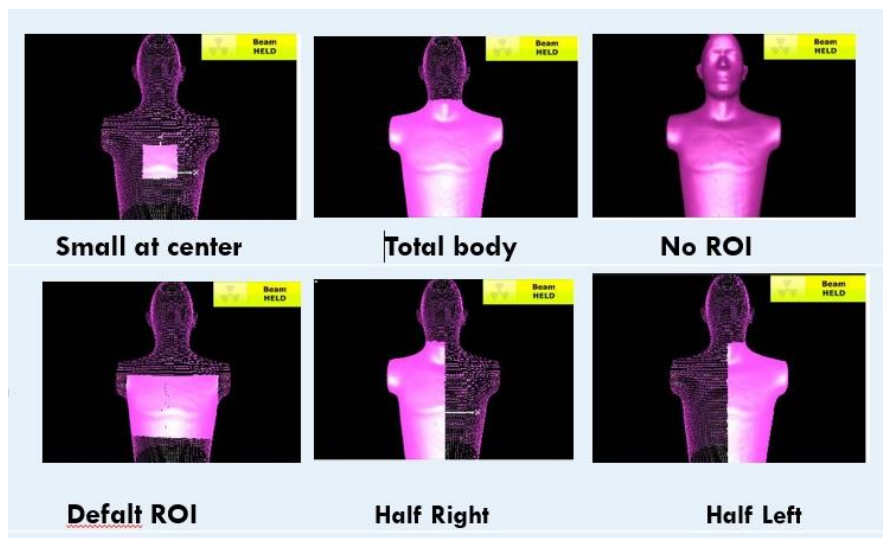


Figure 4.11 ROI conditions for various regions of interest setup.

4.2.1.7 Couch angle effect

At least 2 camera pods were possible to generate 3D surface image. Each pod must angle by 120 degree with another; however, there was the problem of gantry blockage at some angles. The third camera pod was added to solve this problem. The couch angles may have effect to the process of 3D surface image generating because the camera to surface distance will change with changing couch angle then the couch angle effect was needed to study. The rando phantom was set as the treatment patient position and position reported every 10 degree couch angle by AlignRT with moving full rotation as illustrated in figure 4.12. The same phantom position, bright room light condition, mid skin tone protocol and small ROI were acquired. The displacements of phantom position results along vertical, longitudinal and lateral detected by AlignRT were recorded.



Figure 4.12 The phantom setting up for couch angle effect test at (a) 135 and (b) 270 degree couch angle.

4.2.1.8 Time effect

The using time of the AlignRT system contribute to the higher temperature of camera that may affect to 3D surface image generating. This test was study by placing the phantom on the treatment couch and observed the displacement error of 3D surface image in every 30 minute for a total time of 330 minute (this is more than the time to use in clinical). The displacement errors on time effect were reported in vertical, longitudinal and lateral direction.

4.2.2 The correlation between AlingRT and CBCT

At present, the CBCT has been used as the standard IGRT to verify the patient position before treatment. The AlignRT is a new concept applied to verify the patient position in both before and during treatment. The correlation between AlignRT and CBCT is important part to evaluate. However, the accuracy of couch position indicator is an important part to verify before performed this test. To verify the accuracy of couch position indicator, the source to surface distance was set at 100 cm and notices the couch indicators in vertical, longitudinal and, lateral directions. Then the couch was moved to the known distance of -50, -20, -10, -5, 0, 5, 10, 20, and 50 mm in all directions according to the accurate measurement tape. The shifted of couch positions were read on the in-room monitor and the results were recorded. For the correlation between AlignRT and CBCT effect, the rando phantom was scanned at chest region by CT simulator scanner with 120 kVp, 2.5 mm slice thickness with automatic mAs setting. The image data were exported to Eclipse treatment planning system (TPS). The plan with setup and CBCT fields was created and exported to treatment workstation. The phantom was set on the treatment couch as the treatment patient position by using laser systems to achieve the same position as setting in the CT simulator room with the same origin point (0, 0, and 0 mm in vertical, longitudinal and lateral directions respectively) of treatment couch and performed the CBCT and AlingRT as illustrated in figure 4.13. The 3D surface image from 0, 0, 0 mm couch position was set as the reference image. Then the couch was moved to various known couch shift values of -50, -40, -30, -20, -10, -5, -3, -2, -1, 0, 1, 2, 3, 5, 10, 20, 30, 40 and 50 mm in vertical, longitudinal and lateral directions according to displayed couch value on the in-room monitor that was verified during monthly machine quality control. The automatic matching software was chosen to detect the couch deviation by comparing the CBCT image with planning CT image, while the AlignRT can detect the couch shift by comparing the 3D real-time image to reference CT images. The deviation of phantom position of every distances of couch shifted can be detected by AlignRT and CBCT, however, the CBCT has the limitation of automatic couch shift direction in the range of ± 20 mm. The errors of phantom position in every couch position along vertical, longitudinal and lateral detections detected by AlignRT and CBCT were recorded and compared.



Figure 4.13 The set up condition for correlation between AlignRT and CBCT.

4.2.3 Clinical application

The 11 breast cancer patients who treated by DIBH technique with the application of AlignRT were randomly selected to determine the patient setup error before treatment and patient movement during treatment in term of systematic and random errors concept. A total of 1500 reports assessed by AlignRT were performed in daily captured before and during treatments.

4.2.3.1 Patient preparation and planning

For DIBH breast cancer treatment, the patients were setup in supine position on breast board with both hands up over head with foot support. The original position on skin marked was set according to the laser projecting for patient positioning. The deep hold inspiration was practiced before performing CT- scan to make sure that patient could be continued until finishing treatment. The patients were scanned from GE CT simulator with 2.5 mm slice and images were exported to TPS in both free breathing and DIBH series. The target and critical structures included heart and lung were delineated by experienced radiation oncologist. The 3D plan of 6 MV photon with 2 fields of medial and lateral tangential fields was calculated following RTOG breast protocol for normal tissue constraints. The four edges of tangential field size were limited by the breast protocol, the superior edge was opened over the breast

tissue for 15-20 mm to compensate for breathing motion, the inferior edge was limited by the lung that not included lung tissue more than 20 mm, upper and lower edge was covered to base of breast tissue plus 20-30 mm. The dose prescriptions were 50 Gy in 25 fractions with the daily fraction dose of 2 Gy. The patients were treated in Varian TrueBeam linear accelerator equipped with 3D surface tracking system.

4.2.3.2 3D surface tracking system clinical protocol

The laser and skin marked established during simulation process was used for the daily pre-treatment setup. At the first fraction, the 3D surface image was generated by AlignRT to compare with the standard image of CT planning image. When the both images were matched together in the correct position, the captured surface image was generated by AlignRT to use as a reference image for the next repositioning. Because the captured surface image is a real time imaging system, the difference from CT surface image was generated by interpolating from adjacent slice data then using the captured surface image as reference image will be more accurate than using CT surface image. Furthermore, the AlignRT was used to monitor the patient position during treatment by tracking to chest wall. The display monitor of AlignRT showed the patient displacement in 6 directions of vertical, longitudinal, lateral, rotation, yaw and pitch as shown in figure 4.14. However, due to the limitation of couch movement, this study considered in only first three directions. The treatment machine was stopped treating by AlignRT when the displacement error was out of the setting error threshold range and could be treating again when the displacement error turn in the threshold range. The patients' setup errors as inter- and intra-fraction motion were performed using daily reported of AlignRT before and during treatment, respectively. For during treatment situation, the couch shift deviations were recorded 6 times for treatment session. The 3D surface image generated by AlignRT was registered with CT planning to obtain the shifts in the vertical, longitudinal and lateral directions for acquiring movement verification.

4.2.3.3 Statistical analysis for clinical application

The first reported of AlignRT before irradiation was used to calculate the setup error (interfraction motion) while another reported during irradiation (6 times) were used to determine the patient movement (intrafraction motion). Each report composed of the error in vertical, longitudinal and lateral

directions. The average shifted in patient movement during treatment for each patient was calculated.

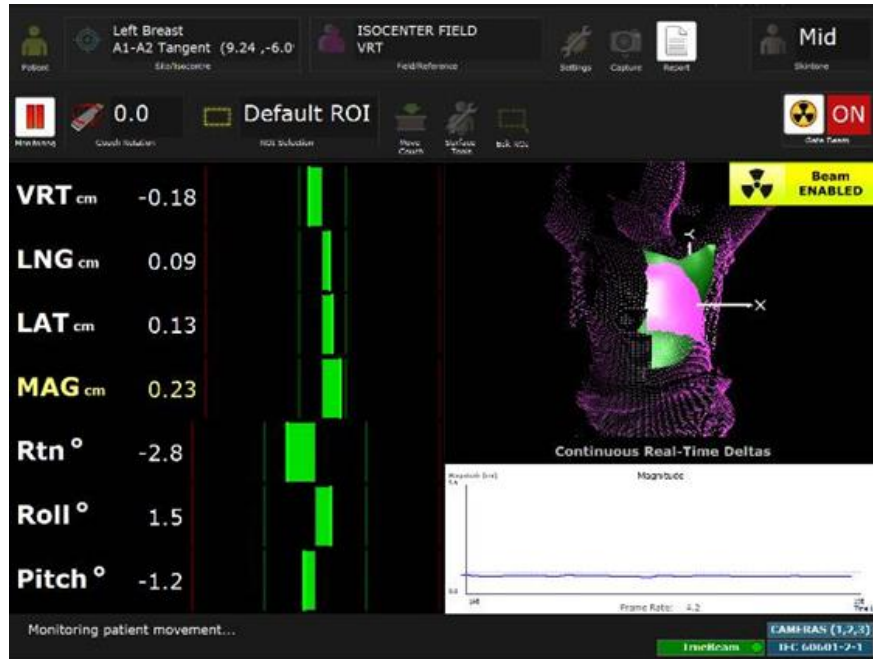


Figure 4.14 Screen capture of AlignRT report.

The mean and SD of the systematic and random errors of individual and population were calculated. The systematic error of population was represented by the standard deviation of mean of each patient, while the random error of population was defined by the mean error of standard deviation for individual patient. The total systematic and total random error can be calculated from the root mean square for setup and patient movement as express in equation (3.1) and (3.2).

$$\Sigma^2_{tot} = \Sigma^2_{setup} + \Sigma^2_{Patient\ motion} \dots \dots \dots (3.1)$$

$$\sigma^2_{tot} = \sigma^2_{setup} + \sigma^2_{Patient\ motion} \dots \dots \dots (3.2)$$

; When Σ is systematic error and σ is random error.

CHAPTER V

RESULTS

5.1 The characteristics of AlignRT

5.1.1 Repeatability of camera calibration

The results of repeatability of camera calibration are shown in table 5.1. The difference data after compared between real-time 3D surface position and reference image were ranged from -0.2 to 0.2 mm for all directions.

Table 5.1 The displacement of phantom position between captured image and reference images (ART_S and CT_S) for repeatability image effect.

Number	ART_S			CT_S		
	Vertical (mm)	Longitudinal (mm)	Lateral (mm)	Vertical (mm)	Longitudinal (mm)	Lateral (mm)
1	0.0	0.0	0.0	0.0	0.0	-0.1
2	0.0	0.0	0.1	0.0	0.0	0.0
3	0.0	0.0	0.1	0.0	0.0	0.0
4	0.0	0.0	0.0	0.0	0.2	0.0
5	0.0	0.0	0.1	0.0	0.1	0.0
6	0.0	0.0	0.0	0.0	0.0	-0.2
7	0.0	-0.1	0.0	0.0	0.0	0.0
8	0.0	0.0	0.1	0.0	0.0	0.0
9	0.0	0.0	0.1	0.0	0.0	0.0
10	0.0	-0.1	0.1	0.0	0.2	0.1

5.1.2 Reproducibility of camera reading

The results of reproducibility of camera calibration along 30 day are shown in table 5.2. The difference value of phantom position compared with ART_S reference image were ranged from -0.8 to 1.6 mm for all directions. The average and standard deviation of shift in vertical, longitudinal and lateral were 0.14 ± 0.32 , 0.44 ± 0.56 and -0.01 ± 0.4 mm, respectively.

Table 5.2 The reproducibility of camera reading of ART_S reference image.

No.	ART_S			No.	ART_S		
	Vertical (mm)	Longitudinal (mm)	Lateral (mm)		Vertical (mm)	Longitudinal (mm)	Lateral (mm)
1	-0.2	0.3	-0.4	16	0.6	0.3	0.1
2	0.2	0.5	0.0	17	-0.1	0.0	-0.6
3	0.2	0.6	0.0	18	0.0	0.8	0.0
4	-0.1	0.4	-0.3	19	0.4	0.9	-0.1
5	0.0	0.3	0.2	20	0.4	0.2	0.1
6	0.3	0.7	0.0	21	-0.1	-0.7	0.3
7	-0.4	0.6	-0.3	22	0.3	0.5	0.1
8	-0.3	0.2	-0.8	23	0.5	0.8	-0.4
9	-0.2	0.3	0.0	24	0.1	0.4	0.1
10	0.3	1.6	0.3	25	0.3	0.3	0.0
11	-0.1	0.4	-0.3	26	0.8	0.2	0.5
12	-0.5	0.3	0.9	27	-0.2	0.3	0.0
13	0.3	1.3	-0.2	28	0.3	0.7	0.2
14	0.1	1.6	-0.7	29	0.7	0.5	0.0
15	0.3	-1.3	1.1	30	0.4	0.2	-0.1

5.1.3 Gantry angle effect

Table 5.3 and table 5.4 present the results of detected shift during rotated the gantry angle of real-time image in every 10 degree to the full rotation compared with ART_S and CT_S reference images, respectively.

Table 5.3 The values of setup error detected by the AlignRT system during rotate gantry to full rotation used the ART_S for reference image.

Gantry angle (Degree)	ART_S			Gantry Angle (Degree)	ART_S		
	Vertical (mm)	Longitudinal (mm)	Lateral (mm)		Vertical (mm)	Longitudinal (mm)	Lateral (mm)
10	-0.1	-0.1	0.0	190	-0.2	-0.1	0.1
20	-0.1	-0.1	0.0	200	-0.1	-0.1	0.1
30	-0.1	-0.1	0.0	210	-0.2	-0.2	0.2
40	-0.1	0.0	0.0	220	-0.2	-0.2	0.2
50	-0.1	-0.1	0.0	230	-0.2	-0.3	0.2
60	-0.1	-0.1	0.0	240	-0.2	-0.2	0.2
70	-0.1	-0.1	0.0	250	-0.2	-0.2	0.2
80	-0.1	-0.1	0.0	260	-0.2	-0.2	0.2
90	-0.1	-0.1	0.0	270	-0.2	-0.1	0.0
100	-0.2	-0.1	0.0	280	-0.2	0.0	0.0
110	-0.2	-0.2	0.2	290	-0.2	-0.1	0.0
120	-0.2	-0.3	0.1	300	-0.2	-0.1	0.0
130	-0.2	-0.2	0.2	310	-0.2	-0.1	0.0
140	-0.2	-0.2	0.2	320	-0.2	-0.1	0.0
150	-0.2	-0.2	0.2	330	-0.2	-0.1	0.0
160	-0.2	-0.2	0.2	340	-0.2	-0.1	0.0
170	-0.2	-0.2	0.2	350	-0.2	-0.2	0.0
180	-0.2	-0.1	0.2	360	-0.1	-0.1	0.0

Table 5.4 The value of setup error detected by the AlignRT system during rotate gantry to full rotation used the CT_S for a reference image.

Gantry angle (Degree)	ART_S			Gantry Angle (Degree)	ART_S		
	Vertical (mm)	Longitudinal (mm)	Lateral (mm)		Vertical (mm)	Longitudinal (mm)	Lateral (mm)
10	0.1	0.0	0.0	190	0.0	-0.2	0.2
20	0.1	0.0	0.0	200	0.0	-0.2	0.2
30	0.1	0.0	0.0	210	0.0	-0.2	0.2
40	0.1	0.0	0.0	220	0.0	-0.1	0.2
50	0.1	0.0	0.0	230	0.0	0.0	0.2
60	0.1	0.0	0.0	240	0.0	0.0	0.2
70	0.1	-0.1	0.0	250	0.0	-0.1	0.2
80	0.1	-0.2	0.0	260	0.0	0.0	0.0
90	0.1	-0.2	0.0	270	0.0	0.0	-0.1
100	0.1	-0.2	0.1	280	-0.1	0.0	-0.2
110	0.1	-0.2	0.2	290	-0.1	0.0	-0.2
120	0.1	-0.2	0.2	300	-0.1	-0.1	-0.2
130	0.0	-0.1	0.2	310	-0.1	0.0	-0.2
140	0.0	-0.2	0.2	320	-0.1	-0.1	-0.2
150	0.0	-0.2	0.2	330	-0.1	0.0	-0.2
160	0.0	-0.2	0.2	340	-0.1	0.1	-0.2
170	0.0	-0.2	0.2	350	-0.1	-0.1	-0.1
180	0.0	-0.2	0.2	360	0.0	0.0	0.0

5.1.4 Room light effect

The results of the room light effect are shown in table 5.5. The setup errors of phantom position were detected by the AlignRT system when varying to the 5 brightness conditions and compared with both ART_S and CT_S for the reference image.

Table 5.5 The phantom position error detected by AlignRT comparing with ART_S and CT_S reference image on room light condition.

Room Light type	ART_S			CT_S		
	Vertical (mm)	Longitudinal (mm)	Lateral (mm)	Vertical (mm)	Longitudinal (mm)	Lateral (mm)
1	0.0	0.0	0.0	0.0	0.0	0.0
2	0.0	0.0	0.0	0.0	0.0	0.0
3	0.0	0.0	0.0	0.0	0.0	0.0
4	0.8	0.6	0.5	0.4	0.3	0.4
5	0.9	0.6	0.7	0.5	0.5	0.4

Type 1 = 131.4 lux

Type 2 = 125.3 lux

Type 3 = 123.0 lux

Type 4 = 5.60 lux

Type 5 = 4.78 lux

5.1.5 Skin tone protocol effect

Table 5.6 shows the results of skin tone protocol effect on the real time 3D surface image comparing with ART_S and CT_S reference image on black surface of the Rando phantom, while table 5.7 presents the results from white surface with surface phantom of AlignRT. The deviation detected by AlignRT system was within ± 1.0 mm for both phantom types, reference image, skin tone protocol and all directions.

Table 5.6 The setup error detected to the Rando phantom (black surface) by the AlignRT system used ART_S and CT_S for reference image.

Skin tone protocol	ART_S			CT_S		
	Vertical (mm)	Longitudinal (mm)	Lateral (mm)	Vertical (mm)	Longitudinal (mm)	Lateral (mm)
Fair	-0.2	-0.4	-0.8	-0.2	-0.5	-0.5
Medium	-0.4	-0.6	0.4	-0.5	-0.3	0.2
Dark	-0.3	-0.2	0.2	-0.3	-0.3	0.3

Table 5.7 The setup error detected to surface phantom of AlignRT (white surface) by the AlignRT system used ART_S for reference image.

Skin tone protocol	ART_S		
	Vertical (mm)	Longitudinal (mm)	Lateral (mm)
Fair	-0.1	-0.3	-0.6
Medium	-0.1	-0.5	0.7
Dark	-0.1	-0.6	-0.9

5.1.6 Region of interest effect

The results of the region of interest effect are shown in table 5.8. The detected shift of the Rando phantom position were reported by the AlignRT system after varying to 6 area of region of interest using ART_S and CT_S for the reference image. The detected shifted were vary from -0.5 to 1.2 mm when the region of interest was changed. The largest deviation was detected in case of using small ROI at center.

Table 5.8 The detected shifts of the Rando phantom on different regions of interested selection.

Type of ROI	ART_S			CT_S		
	Vertical (mm)	Longitudinal (mm)	Lateral (mm)	Vertical (mm)	Longitudinal (mm)	Lateral (mm)
1	-0.3	-0.5	0.7	-0.5	-0.3	1.2
2	0.1	0.0	0.0	0.0	-0.1	-0.2
3	0.0	0.0	0.0	-0.1	-0.1	-0.1
4	-0.3	-0.1	0.1	-0.3	-0.2	0.1
5	0.0	-0.1	0.0	0.1	-0.3	0.2
6	0.0	0.1	0.0	-0.1	0.3	0.2

Type 1 = small at center

Type 4 = cover the body at the center

Type 2 = cover all phantom

Type 5 = half left

Type 3 = no ROI

Type 6 = half right

5.1.7 Couch angle effect

Table 5.9 The setup error detected every 10 degree by the AlignRT system during rotate couch angle from -90 to 90 degree compared with both the ART_S and CT_S reference image.

Couch angle (Degree)	ART_S			CT_S		
	Vertical (mm)	Longitudinal (mm)	Lateral (mm)	Vertical (mm)	Longitudinal (mm)	Lateral (mm)
-90	-0.1	0.3	0.1	-0.1	0.2	0.1
-80	0.1	0.8	0.3	0.1	0.5	0.2
-70	0.1	0.9	1.0	0.1	1.0	0.4
-60	0.1	1.0	0.9	0.1	0.9	0.5
-50	0.3	0.8	1.1	0.3	1.0	0.9
-40	0.1	1.0	0.9	0.1	0.6	0.8
-30	0.1	0.8	0.8	0.1	0.7	0.6
-20	0.0	0.6	0.5	0	0.4	0.3
-10	-0.2	0.4	0.3	-0.2	0.3	0.0
0	-0.2	0.0	0.1	-0.2	-0.2	0.1
10	-0.1	-0.5	0.0	-0.3	-0.6	-0.4
20	-0.1	-0.9	-0.5	-0.3	-0.9	-0.7
30	0.0	-1.1	-1.0	-0.4	-0.9	-0.9
40	-0.2	-0.9	-1.2	-0.3	-1.3	-1.3
50	-0.1	-1.1	-1.3	-0.3	-1.1	-1.3
60	-0.1	-1.0	-1.1	-0.3	-0.9	-1.2
70	0.0	-0.5	-0.6	-0.2	-0.6	-0.8
80	-0.1	-0.3	-0.4	-0.2	-0.6	-0.4
90	-0.1	-0.1	-0.1	-0.2	-0.2	-0.1

The results of the couch angle effect are shown in table 5.9. The detected shifts of the Rando phantom position were detected in every 10 degree couch angle when the couch was rotated from 270 (-90) to 90 degree by the AlignRT system

compared with both ART_S and CT_S for reference image. The detected shifts varied from -1.5 to 2.0 mm during rotating couch when ART_S was used as the reference image, while the shift was in the range between -2.1 and 1.8 mm when CT_S was selected for the reference image.

5.1.8 Time effect

The results of time effect studied from detected the replacement error in every 30 minutes in the same position for a total time of 330 minute is shown in table 5.10. The maximum shift was detected at longitudinal direction of only -0.5 mm.

Table 5.10 The displacement error detected by the AlignRT on time effect compared with the ART_S reference image.

Time (min)	ART_S		
	Vertical (mm)	Longitudinal (mm)	Lateral (mm)
30	-0.1	0.0	0.2
60	-0.1	-0.4	0.1
90	-0.2	-0.4	0.2
120	-0.1	-0.5	0.1
150	-0.2	-0.2	0.0
180	-0.1	-0.2	0.1
210	-0.2	-0.2	0.2
240	-0.1	-0.2	0.1
270	-0.2	-0.4	0.2
300	-0.1	-0.4	0.2
330	-0.1	-0.5	0.2

5.2 The correlation between AlignRT and CBCT

The results of mechanical check of the couch indicator are shown in table 5.11. The maximum differences between known couch shift and actual couch position were only 0.2, 0.2 and 0.1mm error in lateral (at -5.0 mm shift), longitudinal (at -10.0 mm shift) and vertical (at -10 mm shift), respectively.

Table 5.11 Couch position value between known couch and actual position.

Known Couch shift (mm)	Actual couch position (mm)		
	Vertical	Longitudinal	Lateral
-50.0	-50.0	-50.0	-50.0
-20.0	-20.0	-20.0	-20.0
-10.0	-9.9	-10.0	-10.0
-5.0	-5.0	-5.0	-5.2
5.0	5.0	4.9	5.0
10.0	10.0	9.8	9.9
20.0	20.0	19.9	20.0
50.0	50.0	49.9	50.0

The position differences in vertical, longitudinal and lateral directions from the AlignRT system and CBCT compared with known couch shifts are illustrated in table 5.12. The maximum detected shift of AlignRT and CBCT compared with known couch shifts was 0.2 mm and 0.4 mm in vertical, 0.3 mm and 0.7 mm in longitudinal, and 0.2 mm and 0.4 mm, respectively. The correlation factor of AlignRT vs known couch shifts, CBCT vs known couch shifts and AlignRT vs CBCT in each direction calculated from Pearson correlation formula is shown in table 5.13.

Table 5.12 The displacement errors in three major directions detected by the AlignRT system and with the automatic matching software of CBCT (Version 2 MR) compared with known couch shifts.

Known couch shift (mm)	AlignRT			CBCT		
	Vertical (mm)	Longitudinal (mm)	Lateral (mm)	Vertical (mm)	Longitudinal (mm)	Lateral (mm)
-50.0	-49.8	-49.7	-50.4	-	-	-
-30.0	-30.0	-30.7	-30.2	-	-	-
-20.0	-20.0	-20.3	-20.0	-20.3	-20.0	-20.1
-10.0	-10.2	-10.1	-9.8	-10.0	-10.1	-10.0
-5.0	-5.2	-5.0	-4.9	-5.0	-4.9	-5.0
-4.0	-4.0	-3.9	-4.0	-4.1	-3.9	-4.1
-3.0	-3.0	-2.9	-3.0	-2.9	-2.6	-2.8
-2.0	-1.9	-1.7	-2.2	-1.6	-2.3	-2.2
-1.0	-1.0	-1.0	-1.0	-1.3	-0.7	-1.1
0.0	0.0	0.0	0.0	0.0	0.0	0.0
1.0	1.1	1.1	1.1	1.1	1.3	0.9
2.0	2.0	2.0	2.0	2.4	2.6	1.7
3.0	3.1	3.1	3.1	2.7	3.3	2.8
4.0	4.0	4.1	4.0	3.9	3.9	3.9
5.0	5.1	5.0	5.1	5.2	5.1	5.1
10.0	9.9	10.1	10.1	9.8	10.0	10.2
20.0	20.0	19.9	20.1	19.9	20.1	20.4
30.0	30.1	29.9	31.0	-	-	-
50.0	50.1	50.2	51.7	-	-	-

Table 5.13 The correlation factor calculated from Pearson correlation formula to illustrate relationship among the AlignRT system and the CBCT system and known couch shift values.

Relationship	Correlation factor (R)
AlignRT vs Couch shift (Ver.)	0.99999
AlignRT vs Couch shift (Lng.)	0.99996
AlignRT vs Couch shift (Lat.)	0.99990
AlignRT vs CBCT (Ver.)	0.99873
AlignRT vs CBCT (Lng.)	0.99974
AlignRT vs CBCT (Lat.)	0.99952
CBCT vs Couch shift (Ver.)	0.99874
CBCT vs Couch shift (Lng.)	0.99963
CBCT vs Couch shift (Lat.)	0.99952

5.3 Clinical application

The calculated mean and SD of inter and intra fraction motion for individual patient and the raw data of all cases are demonstrated in the Appendix II. The systematic error of population was represented by the standard deviation of mean of each patient, while the random error of population was defined by the mean error of standard deviation for individual patient. The calculated systematic and random error of inter and intra fraction errors for the patients population in vertical, longitudinal and lateral directions of LMT and LLT fields are illustrated in table 5.14 The interfraction motion showed higher value than intrafraction motion in almost all directions.

Table 5.14 The population systematic and random error for inter-and intrafraction of LMT and LLT field

Field	Type of error	Interfraction (mm)			Intrafraction (mm)		
		Ver.	Lng.	Lat.	Ver.	Lng.	Lat.
LMT	Systematic error	0.37	0.38	0.42	0.20	0.20	0.12
	Random error	1.12	1.10	1.06	0.49	0.51	0.32
LLT	Systematic error	0.37	0.32	0.54	0.26	0.36	0.10
	Random error	1.09	1.12	1.18	0.46	0.64	0.29

The root mean square of error was performed to combine the effect of inter-and intrafraction motion and the results of total systematic and random errors are shown in table 5.15.

Table 5.15 The combined effect of inter- and intrafraction motion for systematic and random errors

Type of Error	LMT (mm)			LLT (mm)		
	Ver.	Long.	Lat.	Ver.	Long.	Lat.
Systematic error	0.43	0.43	0.44	0.45	0.48	0.55
Random error	1.23	1.21	1.11	1.18	1.29	1.22

CHAPTER VI

DISCUSSION AND CONCLUSIONS

6.1 Discussion

6.1.1 The characteristic of AlignRT

6.1.1.1 Repeatability of camera reading

The repeatability effect of AlignRT reading was studied by comparing the phantom position between real-time 3D surface image and reference image with continuous detection for 10 times. When the ART_S was used for reference image, the displacement was within 0.1 mm, while the error was increased up to ± 0.2 mm when the CT_S was used as the reference image. The higher error of CT_S reference may be due to including of set up uncertainty, however, these displacements were very small and can be referred that the AlignRT system shows very high precision of camera reading.

6.1.1.2 Reproducibility of camera reading

The reproducibility effect of AlignRT reading was studied by comparing the phantom position between real-time 3D surface image and reference image with the new setup every day for a total of 30 days. The range of displacement error between 3D surface image and reference image was -0.8 to 1.6 mm for all directions. The mean error was 0.14 ± 0.32 mm, 0.44 ± 0.56 mm and -0.01 ± 0.4 mm in vertical, longitudinal and lateral direction, respectively. The largest uncertainty was found in the longitudinal direction. The result was the same trend as Olga Gopan[31] studied that evaluated the accuracy of a 3D surface imaging systems for patient setup in rigid body. They showed the mean error of 0.04 ± 0.03 mm, 0.14 ± 0.14 mm and 0.05 ± 0.06 mm in vertical, longitudinal and lateral direction, respectively.

6.1.1.3 Gantry angle effect

The displacement error was detected during rotate the gantry by every 10 degree for full rotation. The 3D surface image compared with both CT_S and ART_S surface reference images can be displayed in figure 6.1 and figure 6.2.

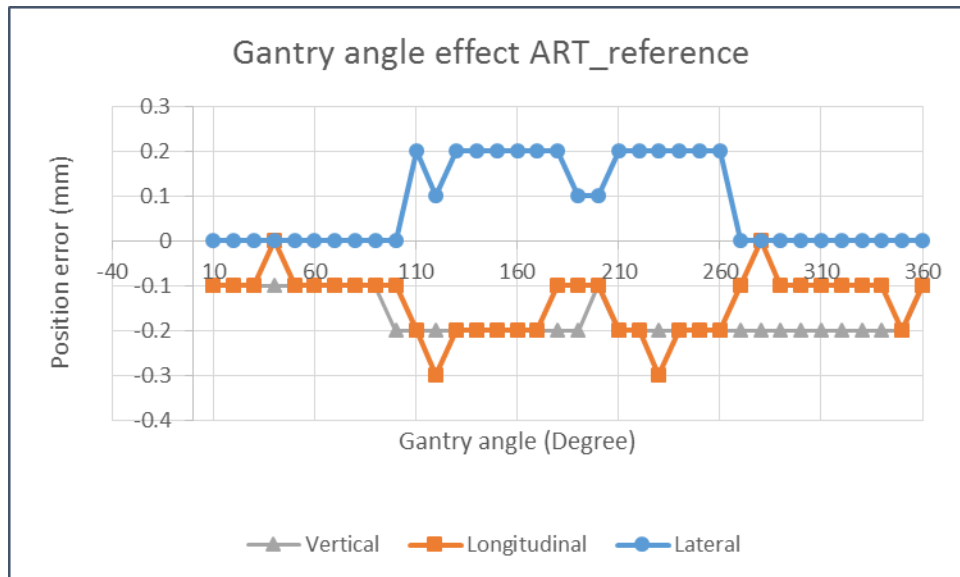


Figure 6.1 The displacement errors during rotate the gantry between 3D surface image and ART_S surface image.

When the ART_S was used as the reference image, the range of displacement error between 3D surface image and reference image was -0.3 to 0.2 mm. The larger uncertainty was detected in the half of lower part of gantry angle in range of 100 and 260 degree for all directions; however, these errors were very small. In case of comparing with CT_S reference image, it showed the same trend as comparing with ART_S reference image. The position uncertainty in all directions was only within 0.2 mm shifted. The result was the same as Peng et al studied [30] who evaluated the gantry blockage effect and they showed the results of, displacement variance of 0.4 mm for both the ART_S and CT_S references. It can be concluded that when the 3 camera pods were used, there was no gantry angle effect to the positioning error for tracking of 3D surface generating.

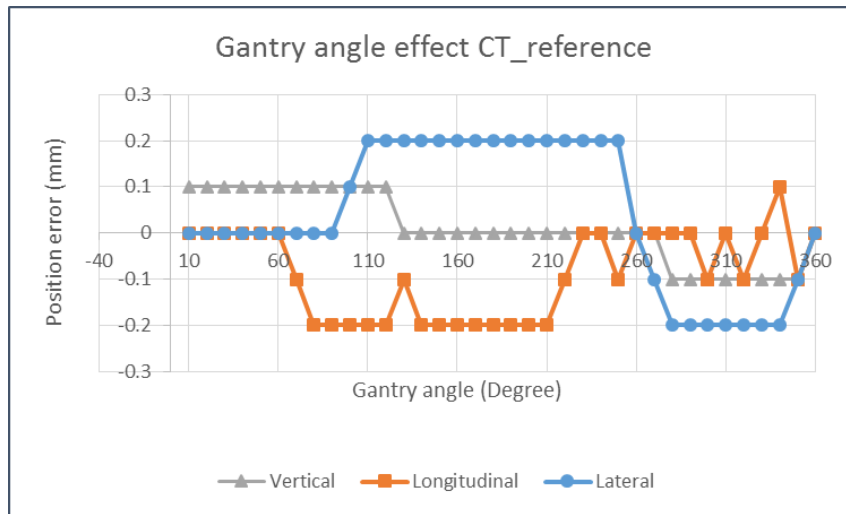


Figure 6.2 The displacement errors during rotate the gantry between 3D surface image and CT_S surface image.

6.1.1.4 Room light effect

Due to the limitation of light switches in treatment room, the brightness of room light can be divided into high and low intensity levels. At the bright room condition (level 1-3) with the brightness of 131.4-123.0 lux, the displacement error was not detected. This may be due to the same brightness condition as the monthly calibration process. When the room become dark (level 4-5) with brightness of 5.60-4.78 lux), the larger uncertainty of phantom position was found. When turn off the light bulbs in the room, the largest errors of 0.9 mm was detected in vertical axis with ART_S reference image. This error is in the accepted level. However, to reduce the error as much as possible, the bright room condition was recommended. The result of Peng[30] showed the effect on registration uncertainty for the different levels of room lighting of less than 0.2 mm. The results of this study differ from Peng studied due to the difference of intensity of room light levels.

6.1.1.5 Skin tone protocol effect

For the skin tone protocol effect, when the rando phantom was represented as the patient in dark skin, the fair skin tone protocol presented the highest detection uncertainly in both comparing both ART_S and CT_S reference images, while the dark skin tone protocol gave the lowest detection uncertainly in both ART_S and CT_S reference images. When the surface phantom of AlignRT was used as the patient in bright skin, the fair skin tone protocol displayed the lowest in positioning

error and vice versa in case of dark skin tone protocol. Therefore, the skin tone protocol should be matched with skin tone for each patient because the skin tone protocol of AlignRT system was designed to adjust intensity of infrared for optimal with patient's skin tone to increase accuracy of image registration.

6.1.1.6 Region of interest effect

For ROI effect, the small error was detected when the large ROI was used and the largest error was found in case of small ROI at center. Because the displacement error was calculated from the mean of whole error in ROI then if the ROI was finite, the small error may have more effect than the same error in large region. The ROI covered lesion area should be selected to increase the accuracy of the displacement errors. These result agree with research of Peng et al.[30] who reported the average registration variances of ROI selected effect of 0.32 ± 0.2 mm. The results showed that the optimal ROI region reference would provide the minimum registration uncertainty.

6.1.1.7 Couch angle effect

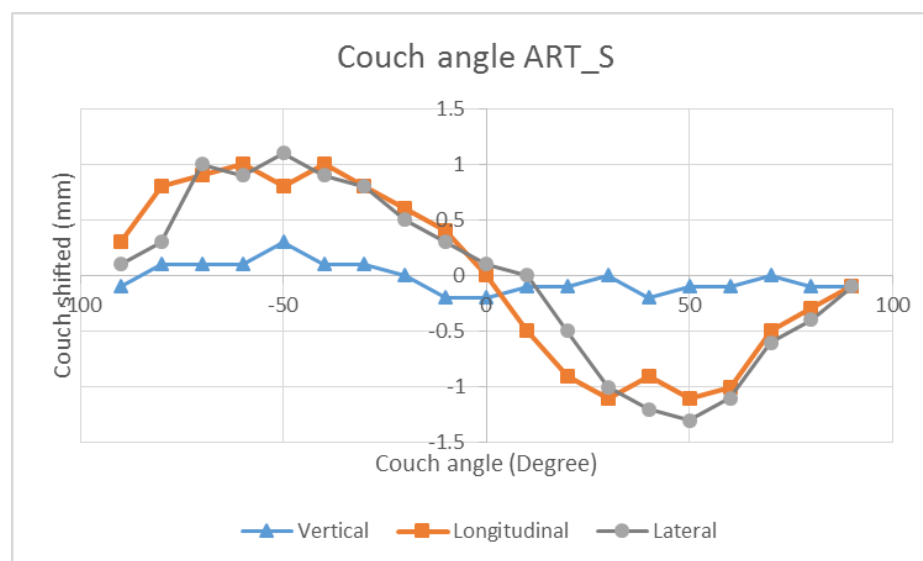


Figure 6.3 The graph of displacement error on various couch angle compared with ART_S reference image in vertical, longitudinal and lateral directions.

The couch location at zero degree was the original position, and then the couch was rotated on the left and right side in every 10 degree to evaluate the effect 3D surface tracking on couch angle. From the result in table 5.9, it can be presented in figure 6.3 and 6.4 for comparison between the real-time 3D surface image and both ART_S and CT_S reference images, respectively. Figure 6.3 shows the

position error detected when rotate the couch and compared the real- time image with ART_S reference image. The longitudinal and lateral direction had the same trend of couch shifted that the maximum error was detected at + and – 45 degree angle, while the vertical direction was no impact on couch angle effect.

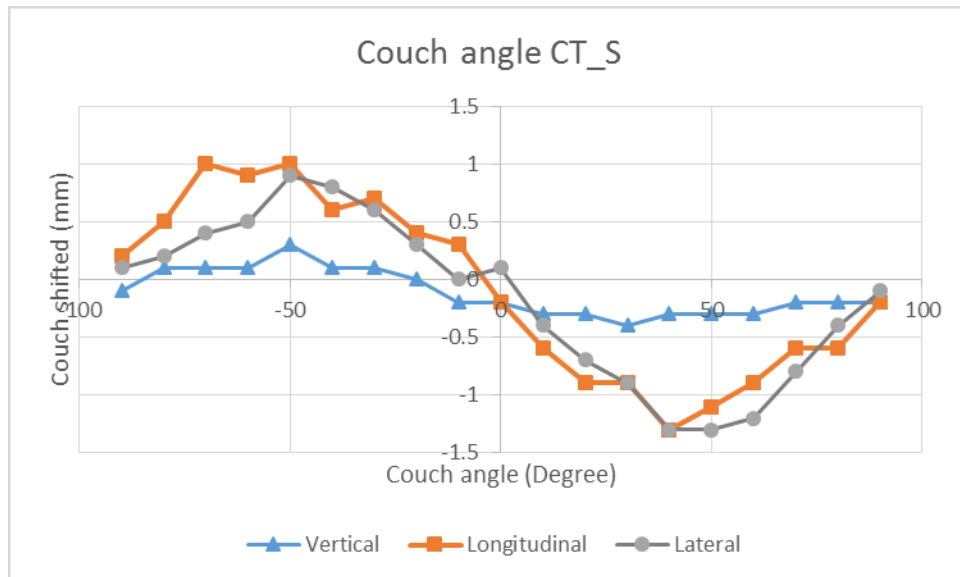


Figure 6.4 The graph of displacement error on various couch angle compared with CT_S reference image in vertical, longitudinal and lateral directions.

The figure 6.4 that used CT_S as the reference image showed the same pattern of the result with ART_S reference image. In both reference images, the largest error was detected at around -40 to -60 and 40 to 60 degree couch angle because these two angles are the largest distance away from one lateral camera.

6.1.1.8 Time effect

Peng studies [30] concluded when the camera was continuous used, the temperature camera will be increased that may affect to the making of 3D surface image. In this study, when time increases, the detection uncertainly was not increase in all directions. The maximum error of ± 0.2 mm was detected in vertical and lateral directions, while the error to -0.5 mm was detected in longitudinal direction. It seems to be the effect was not occurred and not impacted to the creation of real-time 3D surface image that oppose with the time effect theory. The reason is this experiment was periodically performed in every 30 minutes for 330 minutes that was not real continuous used.

6.1.2 The correlation between AlignRT and CBCT

For the accuracy of couch movement testing, the maximum differences between known couch shift and actual couch position were only 0.2 mm error in lateral and longitudinal axes and only 0.1 mm in vertical axis. The specification of the couch traveling shall coincide with the digital display within ± 2 mm according to the Varian recommendation, therefore the very good agreement results were actually obtained and can be confirmed that this mechanical movement of this treatment couch is very accurate.

With the new IGRT concept of AlignRT, the determining of correlation between AlignRT and CBCT is necessary to perform. The automatic couch shifted registration software in CBCT has the limitation at ± 2.0 cm, while AlignRT has no limit in this scenario. At the range of ± 2.0 cm couch shifted, the detection of couch shifted was comparable for CBCT and AlignRT system. At very small shifted in millimeter range, AlignRT resemble better than CBCT in the result. At 5 cm couch shift, AlignRT showed the couch shifted error more than 2 mm in lateral direction. Therefore, the couch shifted from 5 cm. should not be used with accuracy of 1 mm.

If the Pearson correlation factor (R) was chosen to consider the relationship of couch shift among AlignRT system, CBCT system and real couch shifted value, the R factor of 1.00 was the ideal represent that the data from two systems has the relationship to each other.

The data from AlignRT showed the excellent agreement with real couch shift with the correlation factor close to ideal value in all directions, while the correlation between CBCT detected and real couch shift were also good agreement with the R factor larger than 0.9995 in all directions. The result from AlignRT was very good relationship with the results from CBCT with the R factor more than 0.9990 in all directions. It can be implied that AlignRT system can be applied as a new IGRT system with accuracy in the same level as CBCT system.

6.1.3 Clinical application

There are many researches studied about 3D surface tracking system (AlignRT) to verify patient setup uncertainty published over a few years ago [9, 11, 32, 33] and demonstrated that the system could improve the precision of patient's setup

position on breast cancer radiotherapy treatment. In this study, the AlignRT was able to analyze the systematic error and random error in a level of sub millimetre. From 11 patients of 454 images with 2,724 reports tracked before and during treatment, the effect of interfraction motion as the patient setup error was about 2 times higher than the effect of intrafraction motion as the patient movement during treatment. The DIBH technique with AlignRT can reduce the cause of chest wall motion during treatment. When combining the effect of inter-and intrafraction motion via root mean square method, we observed that the total systematic errors were almost 3 times lesser than total random error results in both LMT and LLT fields for all directions. There was no significant difference in result between LMT and LLT fields. The average systematic error for all directions and all fields was 0.46 ± 0.05 mm, while the average random error was 1.21 ± 0.06 mm. The systematic error was less impact than the random error because the using high accuracy of modern machine with suitable immobilization system can reduce the influence from the systematic error while the random error cannot control. The result agreed with the study of Letizia D. et al.[28], who investigated the clinical application of a technique for patient set-up verification in breast cancer radiotherapy based on a 3D surface image registration system. When comparing with the Bert et al.[13] who investigated breast patient setup uncertainty in free breath using AlignRT, the mean displacement of 1.0 ± 1.2 mm was shown while our study had the mean displacement of only 0.39 ± 0.28 mm, this might be due to the using of DIBH technique which the effect of patient movement during treatment was reduced. When the systematic and random errors were compared with Anja Betgen et al.[29] who used 3D surface tracking system to determine set up variability during deep inspiration breath hold radiotherapy for breast cancer patients, the results showed the same trend with our results for intrafraction error which about half of interfraction error. It may be due to the stable in organ movement from DIBH technique.

6.2 Conclusion

The characteristics of the AlignRT system had been studied to verify the factors that may affect to the system before performed in clinical application. This study found that with the new version of 3 camera pods some factors have no effect to

the infrared light such as gantry angle and time factor. However, there are some factors having a minimal effect to the infrared light those are room light level, skin tone protocol, region of interest and couch angle. These effects may influence to the creating of real time 3D surface image and also impact to the detection of displacement error by AlignRT system. The ART_S is recommended to select as the reference image with slightly more accurate and convenience compared with CT_S.

In correlation between AlignRT and CBCT, the result gives very good agreement with each other and also the excellent agreement with known couch shift. From the high correlation result, it can be implied that AlignRT ensure the high accuracy system and can detect the displacement error in the same capability with the CBCT system.

For the clinical application, AlignRT system could be used to determine the patient setup variation in fractionated radiotherapy for left breast cancer patients when using DIBH technique in submillimetre level. The intrafraction motion error from patient setup uncertainty is about half of interfraction motion error, which is less impact due to the stability in organ movement from DIBH. The average systematic and random errors in this study were 0.46 ± 0.05 mm and 1.21 ± 0.06 mm, respectively. The systematic reproducibility is also half of random error because of the high efficiency of modern linac machine that can reduce the systematic uncertainty effectively, while the random error is uncontrollable.

REFERENCES

- 1 Britton KR, Takai Y, Mitsuya M, Nemoto K, Ogawa Y, Yamada S. Evaluation of inter- and intrafraction organ motion during intensity modulated radiation therapy (IMRT) for localized prostate cancer measured by a newly developed on-board image-guided system. *Radiation medicine*. 2005;23(1):14-24.
- 2 Kron T. Reduction of margins in external beam radiotherapy. *Journal of medical physics / Association of Medical Physicists of India*. 2008;33(2):41-2.
- 3 Cancer Research Foundation for National Cancer Institute. *The thai cancer journal*. 2015;35(1).
- 4 Herman MG. Clinical use of electronic portal imaging. *Semin Radiat Oncol*. 2005;15(3):157-67.
- 5 Herman MG, Balter JM, Jaffray DA, McGee KP, Munro P, Shalev S, et al. Clinical use of electronic portal imaging: report of AAPM Radiation Therapy Committee Task Group 58. *Med Phys*. 2001;28(5):712-37.
- 6 Chang J, Yenice KM, Narayana A, Gutin PH. Accuracy and feasibility of cone-beam computed tomography for stereotactic radiosurgery setup. *Med Phys*. 2007;34(6):2077-84.
- 7 Jaffray DA, Drake DG, Moreau M, Martinez AA, Wong JW. A radiographic and tomographic imaging system integrated into a medical linear accelerator for localization of bone and soft-tissue targets. *International journal of radiation oncology, biology, physics*. 1999;45(3):773-89.
- 8 Masi L, Casamassima F, Polli C, Menichelli C, Bonucci I, Cavedon C. Cone beam CT image guidance for intracranial stereotactic treatments: comparison with a frame guided set-up. *International journal of radiation oncology, biology, physics*. 2008;71(3):926-33.

- 9 Bert C, Metheany KG, Doppke K, Chen GT. A phantom evaluation of a stereo-vision surface imaging system for radiotherapy patient setup. *Med Phys.* 2005;32(9):2753-62.
- 10 Li S, Liu D, Yin G, Zhuang P, Geng J. Real-time 3D-surface-guided head re-fixation useful for fractionated stereotactic radiotherapy. *Med Phys.* 2006;33(2):492-503.
- 11 Schoffel PJ, Harms W, Sroka-Perez G, Schlegel W, Karger CP. Accuracy of a commercial optical 3D surface imaging system for realignment of patients for radiotherapy of the thorax. *Phys Med Biol.* 2007;52(13):3949-63.
- 12 Alderliesten T, Sonke JJ, Betgen A, Honnef J, van Vliet-Vroegindeweyj C, Remeijer P. Accuracy evaluation of a 3-dimensional surface imaging system for guidance in deep-inspiration breath-hold radiation therapy. *International journal of radiation oncology, biology, physics.* 2013;85(2):536-42.
- 13 Borst GR, Sonke JJ, den Hollander S, Betgen A, Remeijer P, van Giersbergen A, et al. Clinical results of image-guided deep inspiration breath hold breast irradiation. *International journal of radiation oncology, biology, physics.* 2010;78(5):1345-51.
- 14 Pedersen AN, Korreman S, Nystrom H, Specht L. Breathing adapted radiotherapy of breast cancer: reduction of cardiac and pulmonary doses using voluntary inspiration breath-hold. *Radiotherapy and oncology : journal of the European Society for Therapeutic Radiology and Oncology.* 2004;72(1):53-60.
- 15 Remouchamps VM, Vicini FA, Sharpe MB, Kestin LL, Martinez AA, Wong JW. Significant reductions in heart and lung doses using deep inspiration breath hold with active breathing control and intensity-modulated radiation therapy for patients treated with locoregional breast irradiation. *International journal of radiation oncology, biology, physics.* 2003;55(2):392-406.
- 16 World Cancer Report 2014. World Health Organization. 2014(ISBN 92-832-0429-8):Chapter 5.2.

- 17 2013) ACoSS. Five Things Physicians and Patients Should Question. an initiative of the ABIM Foundation (American College of Surgeons). retrieved 2 January 2013.
- 18 Radiation Therapy. Breastcancerorg. Retrieved 17 November 2015.
- 19 al Se. Human body 3D imaging by speckle texture projection photogrammetry. *Sensor Review* 2000(20:3):218.
- 20 Bert C, Metheany KG, Doppke KP, Taghian AG, Powell SN, Chen GT. Clinical experience with a 3D surface patient setup system for alignment of partial-breast irradiation patients. *International journal of radiation oncology, biology, physics.* 2006;64(4):1265-74.
- 21 Casebow MP, Harris RL, Jarvis RJ. The use of an optical outlining system for weekly on-set verification of patients with carcinoma of the breast. *Radiotherapy and oncology : journal of the European Society for Therapeutic Radiology and Oncology.* 1998;46(1):99-103.
- 22 Cervino LI, Gupta S, Rose MA, Yashar C, Jiang SB. Using surface imaging and visual coaching to improve the reproducibility and stability of deep-inspiration breath hold for left-breast-cancer radiotherapy. *Phys Med Biol.* 2009;54(22):6853-65.
- 23 Riboldi M, Baroni G, Orecchia R, Pedotti A. Enhanced surface registration techniques for patient positioning control in breast cancer radiotherapy. *Technol Cancer Res Treat.* 2004;3(1):51-8.
- 24 Schlegel W BT, Grosu A.L. *New Technologies in Radiation Oncology.* Springer Berlin Heidelberg.
- 25 Thomus B RSU, Wifried D.N, et al. *Image-Guide_IMRT(BookFi.org).* Springer Berlin Heidelberg. 2006;3:22-7.
- 26 raddiologists Trco. On target ensuring geomrtric accuracy in radiotherapy. 2008:11-5.
- 27 Xu F, Wang J, Bai S, Xu QF, Shen YL, Zhong RM. [Interfractional and intrafractional setup errors in radiotherapy for tumors analyzed by cone-beam computed tomography]. *Ai Zheng.* 2008;27(10):1111-6.
- 28 Deantonio L, Masini L, Loi G, Gambaro G, Bolchini C, Krenqli M. Detection of setup uncertainties with 3D surface registration system for conformal

- radiotherapy of breast cancer. Reports of practical oncology and radiotherapy : journal of Greatpoland Cancer Center in Poznan and Polish Society of Radiation Oncology. 2011;16(3):77-81.
- 29 Betgen A, Alderliesten T, Sonke JJ, van Vliet-Vroegindeweij C, Bartelink H, Remeijer P. Assessment of set-up variability during deep inspiration breath hold radiotherapy for breast cancer patients by 3D-surface imaging. Radiotherapy and oncology : journal of the European Society for Therapeutic Radiology and Oncology. 2013;106(2):225-30.
- 30 Peng JL, Kahler D, Li JG, Samant S, Yan G, Amdur R, et al. Characterization of a real-time surface image-guided stereotactic positioning system. Med Phys. 2010;37(10):5421-33.
- 31 Gopan O, Wu Q. Evaluation of the accuracy of a 3D surface imaging system for patient setup in head and neck cancer radiotherapy. International journal of radiation oncology, biology, physics. 2012;84(2):547-52.
- 32 Gierga DP, Riboldi M, Turcotte JC, Sharp GC, Jiang SB, Taghian AG, et al. Comparison of target registration errors for multiple image-guided techniques in accelerated partial breast irradiation. International journal of radiation oncology, biology, physics. 2008;70(4):1239-46.
- 33 Krengli M, Gaiano S, Mones E, Ballare A, Beldi D, Bolchini C, et al. Reproducibility of patient setup by surface image registration system in conformal radiotherapy of prostate cancer. Radiat Oncol. 2009;4:9.

APPENDICES

APPENDIX A

Consent Form

การวิจัยเรื่อง... การหาความคลาดเคลื่อนแบบระบบและแบบสุ่ม จากการใช้ระบบภาพ 3 มิติ
ตรวจจับแบบตลอดเวลาในผู้ป่วยมะเร็งเต้านม

วันที่ให้คำยินยอม วันที่.....เดือน.....พ.ศ.....

ข้าพเจ้า นาย/นาง/นางสาว.....

ที่อยู่.....

ได้อ่านรายละเอียดจากเอกสารข้อมูลสำหรับผู้เข้าร่วม โครงการวิจัยวิจัยที่แนบมาฉบับ

วันที่.....และข้าพเจ้ายินยอมเข้าร่วม โครงการวิจัยโดยสมัครใจ

ข้าพเจ้าได้รับสำเนาเอกสารแสดงความยินยอมเข้าร่วมใน โครงการวิจัยที่ข้าพเจ้าได้ลงนาม และ วันที่ พร้อมด้วยเอกสารข้อมูลสำหรับผู้เข้าร่วม โครงการวิจัย ทั้งนี้ก่อนที่จะลงนามในใบยินยอม ให้ทำการวิจัยนี้ ข้าพเจ้าได้รับการอธิบายจากผู้วิจัยถึงวัตถุประสงค์ของการวิจัย ระยะเวลาของการทำ วิจัย วิธีการวิจัย อันตราย หรืออาการที่อาจเกิดขึ้นจากการวิจัย หรือจากยาที่ใช้ รวมทั้งประโยชน์ที่จะ เกิดขึ้นจากการวิจัย และแนวทางรักษาโดยวิธีอื่นอย่างละเอียด ข้าพเจ้ามีเวลาและโอกาสเพียงพอใน การซักถามข้อสงสัยจนมีความเข้าใจอย่างดีแล้ว โดยผู้วิจัยได้ตอบคำถามต่าง ๆ ด้วยความเต็มใจไม่ ปิดบังซ่อนเร้นจนข้าพเจ้าพอใจ

ข้าพเจ้ารับทราบจากผู้วิจัยว่าหากเกิดอันตรายใด ๆ จากการวิจัยดังกล่าว ข้าพเจ้าจะได้รับการ รักษาพยาบาล โดยไม่เสียค่าใช้จ่าย (และระบุด้วยว่าจะได้รับการชดเชยจากผู้สนับสนุนการวิจัย หรือไม่)

ข้าพเจ้ามีสิทธิที่จะบอกเลิกเข้าร่วมใน โครงการวิจัยเมื่อใดก็ได้ โดยไม่จำเป็นต้องแจ้งเหตุผล และการบอกเลิกการเข้าร่วมการวิจัยนี้ จะไม่มีผลต่อการรักษาโรคหรือสิทธิอื่น ๆ ที่ข้าพเจ้าจะพึง ได้รับต่อไป

ผู้วิจัยรับรองว่าจะเก็บข้อมูลส่วนตัวของข้าพเจ้าเป็นความลับ และจะเปิดเผยได้เฉพาะเมื่อ ได้รับการยินยอมจากข้าพเจ้าเท่านั้น บุคคลอื่นในนามของบริษัทผู้สนับสนุนการวิจัย คณะกรรมการ พิจารณาจริยธรรมการวิจัยในคน สำนักงานคณะกรรมการอาหารและยาอาจได้รับอนุญาตให้เข้ามา ตรวจสอบและประมวลข้อมูลของข้าพเจ้า ทั้งนี้จะต้องกระทำไปเพื่อวัตถุประสงค์เพื่อตรวจสอบความ

ถูกต้องของข้อมูลเท่านั้น โดยการตกลงที่จะเข้าร่วมการศึกษานี้ข้าพเจ้าได้ให้คำยินยอมที่จะให้มีการตรวจสอบข้อมูลประวัติทางการแพทย์ของข้าพเจ้าได้

ผู้วิจัยรับรองว่าจะไม่มีการเก็บข้อมูลใด ๆ เพิ่มเติม หลังจากที่ข้าพเจ้าขอยกเลิกการเข้าร่วมโครงการวิจัยและต้องการให้ทำลายเอกสารและ/หรือ ตัวอย่างที่ใช้ตรวจสอบทั้งหมดที่สามารถสืบค้นถึงตัวข้าพเจ้าได้

ข้าพเจ้าเข้าใจว่า ข้าพเจ้ามีสิทธิ์ที่จะตรวจสอบหรือแก้ไขข้อมูลส่วนตัวของข้าพเจ้าและสามารถยกเลิกการให้สิทธิในการใช้ข้อมูลส่วนตัวของข้าพเจ้าได้ โดยต้องแจ้งให้ผู้วิจัยรับทราบ

ข้าพเจ้าได้ตระหนักว่าข้อมูลในการวิจัยรวมถึงข้อมูลทางการแพทย์ของข้าพเจ้าที่ไม่มีการเปิดเผยชื่อ จะผ่านกระบวนการต่าง ๆ เช่น การเก็บข้อมูล การบันทึกข้อมูลในแบบบันทึกและในคอมพิวเตอร์ การตรวจสอบ การวิเคราะห์ และการรายงานข้อมูลเพื่อวัตถุประสงค์ทางวิชาการรวมทั้งการใช้ข้อมูลทางการแพทย์ในอนาคตหรือการวิจัยทางด้านเภสัชภัณฑ์ เท่านั้น

ข้าพเจ้าได้อ่านข้อความข้างต้นและมีความเข้าใจดีทุกประการแล้ว ยินดีเข้าร่วมในการวิจัยด้วยความเต็มใจ จึงได้ลงนามในเอกสารแสดงความยินยอมนี้

.....ลงนามผู้ให้ความยินยอม
(.....) ชื่อผู้ยินยอมตัวจริง

APPENDIX B

Table B.1 Data of inter fraction for individual patient No.1 in vertical, longitudinal and lateral directions using real- time 3D surface tracking system in breast cancer patient was treated with DIBH technique.

Inter-fraction (Setup error)						
Patient	LMT			LLT		
No.1						
Fraction	Ver	Long	Lat	Ver	Long	Lat
	(cm)	(cm)	(cm)	(cm)	(cm)	(cm)
1	0.1100	-0.2700	-0.1400	0.0400	0.0500	0.1000
2	0.0000	0.0300	0.1600	0.0300	-0.0100	0.0600
3	0.0700	-0.0700	0.2500	-0.1800	0.1800	0.2300
4	-0.1000	-0.1200	0.1000	-0.0200	-0.2100	0.1500
5	-0.1500	0.0800	-0.0200	-0.0800	0.1000	0.0100
6	0.1700	0.0900	0.0400	0.0500	0.0200	-0.1300
7	0.0500	0.0800	-0.0300	0.0000	-0.0700	-0.2300
8	0.0400	-0.0500	-0.1400	0.1500	-0.1300	-0.1200
9	0.2000	-0.1900	-0.0700	0.0800	-0.1400	0.1500
10	0.1400	-0.1700	0.1500	-0.0400	0.0200	0.0500
11	-0.0300	0.0300	0.0200	-0.0900	-0.0600	-0.0800
12	-0.0700	-0.0600	-0.0200	-0.0700	-0.2200	-0.2100
13	-0.0200	-0.2200	-0.0700	-0.1200	-0.1600	-0.1700
14	-0.1900	-0.0900	-0.1000	-0.1300	0.1100	-0.1900
15	-0.1400	0.1600	-0.0200			
16	-0.1000	-0.0900	-0.2700			
17	0.0900	-0.1700	-0.2100			
Mean	0.0041	-0.0606	-0.0218	-0.0294	-0.0406	-0.0600
SD	0.1142	0.1195	0.1312	0.0906	0.1138	0.1629

Table B.2 Data of intra fraction for individual patient No.1 in vertical, longitudinal and lateral directions using real- time 3D surface tracking system in breast cancer patient was treated with DIBH technique.

Intra- fraction (Patient movement)						
Patient	LMT			LLT		
No.1						
Fraction	Vertical	Longitudinal	Lateral	Vertical	Longitudinal	Lateral
	(cm)	(cm)	(cm)	(cm)	(cm)	(cm)
1	-0.0600	0.0450	0.0150	-0.0200	0.0033	-0.0033
2	-0.0100	0.0240	0.0140	-0.0700	0.0580	0.0060
3	-0.0800	0.0660	0.0340	0.0240	0.0000	0.0320
4	0.0217	-0.0017	0.0233	-0.1680	0.1460	0.0100
5	-0.0100	0.0083	0.0167	-0.0200	0.0200	0.0100
6	-0.1100	0.0400	-0.0075	-0.0567	0.0183	-0.0317
7	-0.0650	0.0883	0.0467	-0.0140	0.0220	0.0100
8	-0.0233	0.0167	-0.0067	-0.0317	0.0250	0.0167
9	-0.0583	0.0750	-0.0033	-0.0360	0.0340	0.0000
10	-0.0520	0.0660	0.0200	-0.0720	0.0740	-0.0180
11	-0.0433	0.0300	-0.0150	-0.0633	0.0567	0.0017
12	-0.0640	0.0740	0.0020	-0.0120	0.0420	0.0300
13	-0.0800	0.1317	0.0283	-0.1380	0.1300	0.1400
14	-0.0060	0.0380	0.0240	-0.0300	0.0200	0.0117
15	0.0371	-0.0171	0.0286	-0.0420	0.0680	0.0020
16	-0.0257	0.0343	0.0071	-0.0214	0.0329	-0.0200
17	-0.0367	0.0367	-0.0117			
Mean	-0.0392	0.0444	0.0127	-0.0482	0.0469	0.0123
SD	0.0371	0.0352	0.0171	0.0465	0.0403	0.0367

Table B.3 Data of inter fraction for individual patient No.2 in vertical, longitudinal and lateral directions using real- time 3D surface tracking system in breast cancer patient was treated with DIBH technique.

Inter-fraction (Setup error)						
Patient	LMT			LLT		
No.2						
Fraction	Vertical	Longitudinal	Lateral	Vertical	Longitudinal	Lateral
	(cm)	(cm)	(cm)	(cm)	(cm)	(cm)
1	-0.1700	0.0900	0.2300	-0.0800	-0.0700	0.2600
2	-0.2700	-0.0400	-0.0700	-0.2600	-0.0700	-0.1100
3	-0.2400	0.2200	0.0500	-0.2100	0.2000	0.1300
4	-0.1300	-0.0400	-0.0800	-0.0300	-0.1300	-0.0900
5	-0.1400	-0.1200	-0.0400	-0.1900	-0.1600	-0.1000
6	-0.0100	0.0400	0.0300	0.0300	-0.0400	0.0700
7	0.0000	-0.0800	0.0000	-0.0200	-0.1100	0.0000
8	-0.0100	0.1700	0.2500	0.1100	0.0600	0.2100
9	0.1400	-0.0600	0.1500	-0.1300	0.2400	0.0600
10	-0.0100	0.0300	-0.0400	-0.0500	0.0600	-0.0300
11	-0.2500	0.2100	-0.0300	-0.2500	0.0500	-0.1400
12	0.0800	0.0800	0.1700	0.0400	0.0600	0.2200
13	-0.0400	-0.2400	-0.0300	-0.1300	-0.2400	-0.0200
14	-0.1900	0.1200	0.1300	-0.1400	-0.0900	0.0800
15	-0.0700	-0.0300	-0.1300	-0.0300	-0.0600	0.0100
16	0.0100	-0.0200	-0.0100	0.0800	-0.2600	-0.0800
17	0.0100	0.0300	-0.0400	-0.1900	0.1400	0.0600
18	-0.0900	0.0000	0.0600	-0.2400	0.0400	-0.1200
19	0.0000	-0.0200	-0.1400	-0.1000	0.0000	-0.1300
20	0.0400	-0.0300	-0.0700	0.0200	0.0100	-0.0400
21	0.0200	0.0200	-0.0400	0.0500	0.1800	-0.2400
22	0.1300	0.0800	-0.2000	-0.0800	-0.0400	-0.2400
23	-0.0200	0.0100	-0.1500	0.1500	-0.1300	0.2600

Table B.3 Data of inter fraction for individual patient No.2 in vertical, longitudinal and lateral directions using real- time 3D surface tracking system in breast cancer patient was treated with DIBH technique (cont.).

Inter-fraction (Setup error)						
Patient	LMT			LLT		
No.2						
Fraction	Vertical	Longitudinal	Lateral	Vertical	Longitudinal	Lateral
	(cm)	(cm)	(cm)	(cm)	(cm)	(cm)
24	0.1300	-0.0500	0.1700	-0.1800	0.1500	-0.0600
25	-0.0600	0.0800	0.0800			
Mean	-0.0456	0.0180	0.0100	-0.0763	-0.0088	-0.0017
SD	0.1161	0.1019	0.1202	0.1187	0.1330	0.1433

Table B.4 Data of intra fraction for individual patient No.2 in vertical, longitudinal and lateral directions using real- time 3D surface tracking system in breast cancer patient was treated with DIBH technique.

Intra- fraction (Patient movement)						
Patient	LMT			LLT		
No.2						
Fraction	Vertical	Longitudinal	Lateral	Vertical	Longitudinal	Lateral
	(cm)	(cm)	(cm)	(cm)	(cm)	(cm)
1	-0.0900	0.1100	-0.0025	-0.1020	0.0840	-0.0060
2	0.1060	-0.1520	-0.0700	0.0080	-0.0180	0.0300
3	0.0325	-0.0125	0.0650	-0.0100	0.0167	-0.0033
4	-0.0100	0.0275	0.0175	-0.0500	0.0520	-0.0380
5	-0.0860	0.0680	-0.0100	-0.0420	0.0220	0.0000
6	-0.1033	0.1050	-0.0033	-0.0340	0.0320	-0.0240
7	-0.0150	0.0267	0.0133	-0.0050	0.0133	-0.0200
8	0.0467	-0.0567	0.0050	0.0100	-0.0160	-0.0100
9	-0.0829	0.0943	-0.0886	-0.0020	0.0240	0.0140
10	-0.0029	-0.0257	-0.0314	-0.0080	-0.0100	-0.0340

Table B.4 Data of intra fraction for individual patient No.2 in vertical, longitudinal and lateral directions using real- time 3D surface tracking system in breast cancer patient was treated with DIBH technique (cont.).

Intra- fraction (Patient movement)						
Patient	LMT			LLT		
No.2						
Fraction	Vertical	Longitudinal	Lateral	Vertical	Longitudinal	Lateral
	(cm)	(cm)	(cm)	(cm)	(cm)	(cm)
11	0.0300	-0.0125	0.0225	0.0620	-0.0600	0.0440
12	0.0017	-0.0733	-0.0667	0.0317	-0.0600	-0.0167
13	0.0050	-0.0467	-0.0083	0.0080	0.0020	0.0020
14	0.0167	-0.0283	-0.0017	0.0000	-0.0320	-0.0480
15	0.0460	-0.0560	0.0240	0.0475	-0.0725	-0.0675
16	0.0080	-0.0240	-0.0120	0.0000	0.0080	0.0020
17	0.0100	-0.0280	-0.0260	0.0160	-0.0260	-0.0060
18	0.0275	-0.0100	-0.0200	0.0250	-0.0050	-0.0183
19	-0.0050	-0.0150	-0.0050	0.0060	-0.0440	-0.0240
20	-0.0020	-0.0160	-0.0160	0.0800	-0.0414	0.1000
21	-0.0050	-0.0075	0.0025	0.0020	-0.0040	-0.0180
22	-0.0017	0.0300	-0.0067	0.0140	-0.0440	0.0220
23	-0.0350	0.0038	-0.1900	-0.0380	0.0060	-0.0460
24	-0.0400	-0.0225	-0.0475	0.0275	-0.0200	-0.0200
25	0.0014	-0.0300	-0.0286			
Mean	-0.0059	-0.0061	-0.0194	0.0019	-0.0080	-0.0077
SD	0.0475	0.0578	0.0481	0.0379	0.0371	0.0341

Table B.5 Data of inter fraction for individual patient No.3 in vertical, longitudinal and lateral directions using real- time 3D surface tracking system in breast cancer patient was treated with DIBH technique.

Inter-fraction (Setup error)						
Patient	LMT			LLT		
No.3						
Fraction	Vertical	Longitudinal	Lateral	Vertical	Longitudinal	Lateral
	(cm)	(cm)	(cm)	(cm)	(cm)	(cm)
1	0.1100	-0.0300	-0.0100	0.0100	-0.0500	-0.0400
2	0.0600	-0.0700	0.0600	0.0500	-0.0800	0.1300
3	0.0100	0.0000	0.0600	0.0400	-0.0100	0.1400
4	-0.1000	0.0100	-0.0200	-0.1100	0.0700	0.0900
5	0.0700	0.2500	0.1000	0.0900	0.2500	0.1700
6	-0.0700	0.0300	-0.0300	-0.1500	0.0300	-0.0400
7	-0.1200	-0.0100	0.1400	0.0400	-0.0700	0.3100
8	-0.0200	0.0900	0.0500	-0.0200	0.1500	0.2400
9	0.0100	0.0000	0.0700	0.0100	-0.0400	0.0700
10	-0.0400	0.0200	0.0000	-0.0700	0.0200	-0.0300
11	-0.1300	0.0300	-0.0100	-0.1300	0.0400	0.0100
12	-0.0800	0.2300	-0.0800	-0.1400	0.2700	-0.0400
13	-0.1500	0.0700	0.0900	-0.0600	0.0200	0.1100
14	0.0400	-0.0700	-0.0300	0.1200	-0.1100	0.0500
15	0.0600	-0.0600	0.1700	0.1100	-0.1100	0.2400
16	-0.0100	0.0800	0.1100	0.0400	-0.2300	0.0600
17	-0.0100	-0.1800	0.0700	-0.2100	0.0000	0.1000
18	-0.2300	-0.0600	0.0600	0.0900	0.0500	0.0700
19	0.1300	0.0500	0.0700	-0.0900	0.0000	-0.0100
20	-0.0900	-0.1300	-0.0100	-0.0600	-0.0300	0.0000
21	-0.0800	0.0500	-0.0500			
Mean	-0.0305	0.0143	0.0386	-0.0220	0.0085	0.0815
SD	0.0917	0.1013	0.0659	0.0963	0.1171	0.1015

Table B.6 Data of intra fraction for individual patient No.3 in vertical, longitudinal and lateral directions using real- time 3D surface tracking system in breast cancer patient was treated with DIBH technique.

Intra- fraction (Patient movement)						
Patient	LMT			LLT		
No.3						
Fraction	Vertical	Longitudinal	Lateral	Vertical	Longitudinal	Lateral
	(cm)	(cm)	(cm)	(cm)	(cm)	(cm)
1	-0.0125	0.0250	0.0050	-0.0150	0.0750	0.0450
2	-0.0300	0.0233	0.0033	-0.0340	0.0460	0.0080
3	-0.0717	0.0600	0.0150	-0.0267	0.0333	0.0267
4	-0.0360	0.0540	0.0400	-0.0240	0.0340	-0.0060
5	-0.0980	0.0040	-0.0420	-0.2850	0.0625	-0.0375
6	-0.0620	0.0340	-0.0460	-0.0420	0.0340	-0.0560
7	-0.0160	0.0320	0.0340	-0.0500	0.0360	-0.0060
8	-0.0240	0.0540	0.0320	-0.0300	0.0300	-0.0100
9	-0.0440	0.0080	-0.0140	-0.0075	0.0125	0.0025
10	-0.0420	0.0440	-0.0260	-0.0360	-0.0060	-0.0140
11	-0.0440	0.0260	-0.0020	-0.0860	0.0800	-0.0040
12	-0.0240	0.0340	0.0400	-0.1033	0.1000	-0.0233
13	-0.0680	0.0500	0.0000	-0.0360	0.0260	0.0020
14	-0.0100	0.0300	0.0100	-0.2060	0.0560	-0.0080
15	-0.0200	0.0800	0.0300	0.0160	0.0100	0.0000
16	-0.0300	0.0700	0.0100	-0.0675	0.0400	-0.0250
17	-0.0500	0.1000	0.0100	0.0000	0.0280	0.0100
18	-0.0275	0.0700	0.0150	-0.1040	0.0940	0.0060
19	-0.0540	0.0320	-0.1980			
20	-0.0620	0.0260	-0.0080			
21	-0.0260	0.0320	-0.0040			
Mean	-0.0406	0.0430	-0.0076	-0.0632	0.0440	-0.0050
SD	0.0293	0.0238	0.0469	0.0752	0.0289	0.0226

Table B.7 Data of inter fraction for individual patient No.4 in vertical, longitudinal and lateral directions using real- time 3D surface tracking system in breast cancer patient was treated with DIBH technique.

Inter-fraction (Setup error)						
Patient	LMT			LLT		
No.4						
Fraction	Vertical	Longitudinal	Lateral	Vertical	Longitudinal	Lateral
	(cm)	(cm)	(cm)	(cm)	(cm)	(cm)
1	-0.0500	0.0300	-0.2200	-0.2000	0.1300	-0.1700
2	0.0800	0.2600	0.0400	0.0700	0.1000	0.0300
3	0.0400	-0.1800	-0.0500	-0.2500	0.1700	0.0000
4	0.0400	-0.1800	-0.0500	-0.2500	0.1700	0.0000
5	0.1100	-0.0600	0.2500	-0.0100	0.0300	0.2600
6	-0.0300	-0.0300	0.1500	-0.0800	-0.0300	0.0800
7	0.0400	-0.1500	-0.0100	-0.0300	-0.1800	0.0000
8	-0.0900	0.0200	-0.1100	-0.0400	-0.0900	-0.0600
9	0.0600	-0.1900	0.0100	-0.1500	0.0400	0.0200
10	-0.1800	0.2100	0.1900	-0.1600	0.1600	0.2500
11	0.0500	-0.0900	0.0300	-0.0400	0.0000	0.0700
12	-0.0600	0.0600	0.1100	-0.0700	0.0500	0.1200
13	0.2100	-0.3400	0.0700	-0.0600	0.1400	0.0400
14	-0.0600	0.1300	0.1400			
Mean	0.0114	-0.0364	0.0393	-0.0977	0.0531	0.0492
SD	0.0972	0.1679	0.1254	0.0971	0.1079	0.1154

Table B.8 Data of intra fraction for individual patient No.4 in vertical, longitudinal and lateral directions using real- time 3D surface tracking system in breast cancer patient was treated with DIBH technique.

Intra- fraction (Patient movement)						
Patient	LMT			LLT		
No.4						
Fraction	Vertical	Longitudinal	Lateral	Vertical	Longitudinal	Lateral
	(cm)	(cm)	(cm)	(cm)	(cm)	(cm)
1	-0.0386	0.0514	-0.0129	-0.0325	0.0450	-0.0100
2	-0.0086	-0.0514	0.0214	-0.0067	0.0167	-0.0167
3	-0.0329	0.0257	0.0143	-0.0067	0.0167	-0.0167
4	-0.0329	0.0257	0.0143	-0.0050	0.0100	-0.0050
5	-0.0214	0.0100	-0.0529	-0.0250	0.0150	-0.0375
6	-0.0380	0.0340	-0.0160	-0.0025	0.0200	-0.0100
7	-0.0314	0.0486	-0.0114	-0.0150	0.0275	-0.0175
8	-0.0643	0.0700	0.0200	-0.0100	0.0225	0.0075
9	-0.0683	0.0883	-0.0117	-0.0033	0.0000	-0.0333
10	0.0533	-0.0733	-0.0033	0.0000	-0.0200	0.0000
11	-0.0400	0.0400	0.0250	0.0525	-0.0575	0.0225
12	-0.0040	-0.0140	0.0120	-0.0325	0.0450	0.0300
13	-0.3720	0.3180	-0.0860			
14	-0.0329	0.0157	-0.0014			
Mean	-0.0523	0.0421	-0.0063	-0.0072	0.0117	-0.0072
SD	0.0965	0.0906	0.0308	0.0220	0.0280	0.0201

Table B.9 Data of inter fraction for individual patient No.5 in vertical, longitudinal and lateral directions using real- time 3D surface tracking system in breast cancer patient was treated with DIBH technique.

Inter-fraction (Setup error)						
Patient	LMT			LLT		
No.5						
Fraction	Vertical	Longitudinal	Lateral	Vertical	Longitudinal	Lateral
	(cm)	(cm)	(cm)	(cm)	(cm)	(cm)
1	-0.1300	-0.1500	-0.1200	-0.1700	-0.1300	-0.1300
2	0.0600	-0.0100	0.1400	0.0600	-0.0200	0.1400
3	-0.2300	-0.0500	0.0000	-0.1900	-0.0600	0.0800
4	0.0200	-0.1200	-0.0300	-0.0800	-0.0500	-0.1100
5	-0.0500	0.0400	-0.1200	-0.1100	-0.0800	-0.0800
6	0.1000	-0.0600	0.2800	-0.0700	0.0100	-0.1300
7	0.0600	0.0500	0.0000	0.0500	-0.0400	0.3100
8	0.0200	-0.0800	0.0700	0.1000	-0.0300	0.0000
9	-0.1900	-0.0400	0.1400	0.0100	-0.0500	0.1000
10	-0.0600	-0.0100	0.1500	-0.2100	-0.0500	0.1200
11	0.0500	-0.0200	-0.0600	-0.1100	0.0000	0.1100
12	0.0400	-0.0100	0.0500	0.0100	0.0400	-0.0400
13	-0.0500	-0.2300	0.0300	-0.1600	0.1400	0.0300
14	-0.0600	0.0600	0.1400	0.0200	-0.2500	0.0800
15				-0.1100	0.0700	0.1200
Mean	-0.0300	-0.0450	0.0479	-0.0640	-0.0333	0.0400
SD	0.0991	0.0804	0.1141	0.0991	0.0884	0.1225

Table B.10 Data of intra fraction for individual patient No.5 in vertical, longitudinal and lateral directions using real- time 3D surface tracking system in breast cancer patient was treated with DIBH technique.

Intra- fraction (Patient movement)						
Patient	LMT			LLT		
No.5						
Fraction	Vertical	Longitudinal	Lateral	Vertical	Longitudinal	Lateral
	(cm)	(cm)	(cm)	(cm)	(cm)	(cm)
1	0.0683	0.0283	0.0700	0.0360	0.0000	0.0200
2	0.0160	0.0000	0.0020	0.0220	-0.8060	-0.0040
3	0.0200	-0.0020	0.0080	0.0025	-0.0175	0.0025
4	-0.0150	0.0125	-0.0050	-0.0033	0.0067	0.0067
5	0.0080	-0.0060	0.0180	0.0140	0.0020	0.0280
6	0.0225	-0.0150	0.0175	0.0180	0.0020	0.0580
7	-0.0540	0.0440	0.0040	0.0250	-0.0267	-0.0183
8	0.0150	-0.0167	0.0117	-0.0200	-0.0020	-0.0260
9	0.0000	0.0360	0.0300	0.0200	-0.0060	0.0300
10	0.0100	0.0040	-0.0080	0.0325	-0.0075	0.0400
11	0.0020	0.0100	0.0180	0.0260	-0.0180	0.0260
12	0.0125	0.0050	0.0200	0.0100	0.0020	-0.0160
13	-0.0080	-0.0040	-0.0080	0.0100	-0.0140	-0.0200
14	-0.0060	0.1120	-0.0040	-0.0220	0.0040	-0.0020
15	-0.0140	0.0140	-0.0140	-0.0220	0.0180	0.0080
Mean	0.0065	0.0149	0.0124	0.0122	-0.0629	0.0089
SD	0.0259	0.0320	0.0208	0.0192	0.2074	0.0244

Table B.11 Data of inter fraction for individual patient No.6 in vertical, longitudinal and lateral directions using real- time 3D surface tracking system in breast cancer patient was treated with DIBH technique.

Inter-fraction (Setup error)						
Patient	LMT			LLT		
No.6						
Fraction	Vertical	Longitudinal	Lateral	Vertical	Longitudinal	Lateral
	(cm)	(cm)	(cm)	(cm)	(cm)	(cm)
1	0.0200	-0.0500	0.2600	-0.0700	-0.1900	-0.1800
2	-0.0900	-0.1200	0.1900	-0.1800	-0.0600	0.2200
3	-0.0400	0.1900	0.1000	0.1000	0.0800	0.2900
4	0.2600	0.0700	0.0400	-0.2400	0.3800	-0.0700
5	-0.0900	0.2500	0.1500	0.1000	-0.1400	0.2400
6	0.0900	0.0900	0.0200	-0.1800	0.1300	0.0100
7	-0.0200	0.0800	0.2300	-0.0700	0.0100	0.2500
8	0.0200	0.0400	0.0400	0.1300	0.0300	0.1800
9	0.0800	0.0700	0.1500	-0.0500	0.0600	0.0800
10	-0.1100	0.0400	-0.0700	0.2700	0.0900	0.0900
11	0.1000	0.0500	0.0200	0.1800	0.1000	0.0500
12	0.0700	0.1200	0.1600	0.1000	-0.2400	0.0600
13	-0.1000	0.0300	0.0400	0.0100	0.0700	0.1500
14	0.1600	-0.2300	0.0800	0.1300	-0.1600	0.1200
15	-0.1100	-0.1000	0.1200	-0.1400	-0.0700	0.0800
16	0.1100	-0.0700	0.2200	0.0300	0.0100	0.2600
17	-0.1800	0.1800	-0.1900	-0.0700	0.2300	-0.1600
18	0.2700	0.0100	0.2000	0.0600	0.0600	0.0600
19	0.0700	0.0500	0.2800	-0.1000	0.0100	-0.0300
Mean	0.0268	0.0368	0.1074	0.0005	0.0211	0.0895
SD	0.1257	0.1149	0.1184	0.1380	0.1474	0.1358

Table B.12 Data of intra fraction for individual patient No.6 in vertical, longitudinal and lateral directions using real- time 3D surface tracking system in breast cancer patient was treated with DIBH technique.

Intra- fraction (Patient movement)						
Patient	LMT			LLT		
No.6						
Fraction	Vertical	Longitudinal	Lateral	Vertical	Longitudinal	Lateral
	(cm)	(cm)	(cm)	(cm)	(cm)	(cm)
1	-0.0933	0.0200	-0.0167	0.0167	0.0033	-0.0033
2	-0.0140	-0.0280	-0.0200	-0.0150	0.0450	0.0650
3	0.0680	-0.0962	0.0060	0.0567	0.0533	0.0167
4	-0.2750	0.2400	-0.0450	0.0067	-0.4967	0.0033
5	-0.0325	-0.1450	0.1250	-0.0100	0.0425	0.0500
6	-0.1840	0.1920	0.0420	0.0060	0.1160	0.0160
7	-0.0760	0.0400	-0.0080	-0.0340	0.0420	0.0020
8	-0.0240	0.0860	-0.0140	0.0860	0.0180	0.0140
9	-0.1060	0.0780	-0.0120	-0.0860	0.0920	-0.0240
10	0.1140	0.0540	0.1260	-0.0120	-0.0320	-0.0460
11	-0.0220	0.0140	-0.0280	0.0200	0.0100	0.0180
12	0.0380	-0.0280	0.0020	0.0225	-0.0100	-0.0200
13	0.0720	0.0020	0.0500	0.0880	-0.0320	0.0140
14	-0.0025	0.0000	-0.0175	0.0140	-0.0180	0.0060
15	-0.0150	0.0000	-0.0150	-0.0120	-0.0140	-0.0100
16	0.0075	-0.0050	0.0125	0.0133	0.0067	-0.0167
17	0.0350	0.0350	0.0225	0.0320	0.0260	0.0300
18	0.0120	-0.0180	0.0220	0.0320	-0.0300	-0.0120
19	0.0144	-0.0156	0.0184	-0.0560	-0.1500	0.0260
Mean	-0.0254	0.0224	0.0132	0.0089	-0.0173	0.0068
SD	0.0917	0.0873	0.0462	0.0427	0.1288	0.0262

Table B.13 Data of inter fraction for individual patient No.7 in vertical, longitudinal and lateral directions using real- time 3D surface tracking system in breast cancer patient was treated with DIBH technique.

Inter-fraction (Setup error)						
Patient	LMT			LLT		
No.7						
Fraction	Vertical	Longitudinal	Lateral	Vertical	Longitudinal	Lateral
	(cm)	(cm)	(cm)	(cm)	(cm)	(cm)
1	-0.2000	0.0700	0.0500	-0.0200	0.0800	-0.1100
2	0.0400	-0.0100	-0.0400	-0.0300	-0.0900	-0.0200
3	0.0000	-0.0300	0.0000	-0.1200	0.0200	0.0000
4	-0.0900	0.0000	0.0800	0.0600	0.0500	-0.0900
5	-0.0600	-0.1100	0.0700	-0.0200	-0.0400	0.0100
6	-0.1400	0.0600	-0.0400	0.1300	0.1500	-0.1000
7	0.0000	-0.0300	-0.0200	-0.0800	0.1300	0.0800
8	-0.0300	-0.0100	0.0300	-0.0700	0.1000	-0.1500
9	0.1000	0.1700	-0.1200	0.0900	-0.0300	-0.1300
10	-0.0300	0.0800	0.0600	-0.1600	0.1200	0.1100
11	-0.0600	0.0200	-0.1700	-0.0300	0.0700	0.1900
12	-0.4900	0.1000	-0.0900	0.0600	0.0200	-0.0200
13	-0.0500	0.1800	-0.0700	-0.0500	-0.0400	0.0100
14	0.0600	0.0700	0.2000	0.1100	-0.0600	-0.0900
15	-0.1000	0.1500	0.1000	0.0000	-0.1100	-0.1100
16	-0.1900	0.2200	0.1800	-0.1100	-0.0500	0.0000
17	0.0700	0.0100	0.0100	-0.1500	0.1600	-0.0400
18	-0.0800	0.0400	-0.0200			
19	0.0800	-0.1300	-0.1000			
20	0.1900	-0.0800	0.0700			
Mean	-0.0577	0.0400	0.0055	-0.0229	0.0282	-0.0271
SD	0.1386	0.0985	0.0919	0.0889	0.0869	0.0917

Table B.14 Data of intra fraction for individual patient No.7 in vertical, longitudinal and lateral directions using real- time 3D surface tracking system in breast cancer patient was treated with DIBH technique.

Intra- fraction (Patient movement)						
Patient	LMT			LLT		
No.7						
Fraction	Vertical	Longitudinal	Lateral	Vertical	Longitudinal	Lateral
	(cm)	(cm)	(cm)	(cm)	(cm)	(cm)
1	0.0867	-0.0233	-0.0733	0.0067	-0.0067	0.0167
2	-0.0225	0.0225	-0.0025	-0.0233	0.0167	-0.0333
3	0.0000	0.0000	0.0100	0.0000	-0.0167	0.0167
4	-0.0100	-0.0100	-0.0200	-0.0333	-0.0033	0.0200
5	-0.0175	0.0000	-0.0150	-0.0167	0.0133	0.0067
6	-0.0133	-0.0033	-0.0033	0.0067	-0.0067	-0.0033
7	0.0100	0.0133	-0.0033	0.0400	-0.0300	0.0000
8	-0.0067	-0.0100	0.0000	-0.0575	-0.0025	-0.0425
9	-0.0100	0.0000	0.0000	-0.0700	0.0533	-0.0033
10	-0.0067	-0.0067	0.0000	-0.0600	0.0100	-0.0150
11	-0.0133	-0.0100	-0.0167	0.0443	-0.0271	-0.1229
12	0.2975	-0.2675	-0.1000	-0.0233	0.0067	-0.0100
13	-0.0067	0.0033	-0.0100	-0.0067	0.0100	0.0100
14	-0.0167	0.0133	-0.0033	-0.0200	0.0000	-0.0033
15	-0.0167	-0.0100	-0.0100	0.0250	0.0100	0.0550
16	-0.0100	0.0300	0.0200			
17	-0.0025	0.0050	-0.0125			
18	-0.0071	0.1486	-0.0286			
Mean	0.0130	-0.0058	-0.0149	-0.0125	0.0018	-0.0072
SD	0.0749	0.0751	0.0287	0.0345	0.0200	0.0394

Table B.15 Data of inter fraction for individual patient No.8 in vertical, longitudinal and lateral directions using real- time 3D surface tracking system in breast cancer patient was treated with DIBH technique.

Inter-fraction (Setup error)						
Patient	LMT			LLT		
No.8						
Fraction	Vertical	Longitudinal	Lateral	Vertical	Longitudinal	Lateral
	(cm)	(cm)	(cm)	(cm)	(cm)	(cm)
1	-0.2100	0.0800	0.0700	-0.0400	-0.0100	-0.0300
2	-0.0500	0.0900	0.0400	-0.0800	-0.0400	0.0700
3	-0.1000	0.0600	0.0500	0.0000	-0.0100	0.0200
4	-0.1500	0.0300	0.0400	0.1200	-0.0200	-0.1000
5	-0.0800	-0.0200	0.0400	-0.1200	0.0300	0.0400
6	0.0500	-0.1100	-0.0600	-0.0700	0.0100	-0.1100
7	-0.1700	-0.0100	0.0100	-0.0300	0.1100	0.0000
8	-0.1000	0.0000	0.0500	-0.0200	0.0900	0.1000
9	-0.0500	0.0400	0.0400	0.1100	0.0300	-0.0200
10	-0.1800	0.1100	-0.1300	-0.0700	0.2500	0.0500
11	-0.0400	0.0000	0.0200	0.0900	0.0300	0.0800
12	-0.0500	0.0100	-0.0300	-0.2200	0.1300	0.0400
13	-0.3100	0.2300	0.0900	-0.1000	0.0500	-0.0100
14	-0.0400	0.2000	0.0800	-0.0500	0.2500	0.0800
15	0.0600	-0.0900	0.0300	0.0400	-0.1100	-0.0900
16	-0.2000	0.0400	-0.0500	0.1700	-0.1100	0.1400
17	-0.1700	0.0200	0.0100	-0.0900	-0.0400	0.0300
18	-0.0100	0.1200	0.1500	-0.1000	-0.2300	-0.0600
19	0.2200	-0.1900	0.0100	-0.0300	0.0800	0.0400
20	-0.0700	-0.0400	0.0600	-0.0600	-0.0100	0.0100

Table B.15 Data of inter fraction for individual patient No.8 in vertical, longitudinal and lateral directions using real- time 3D surface tracking system in breast cancer patient was treated with DIBH technique (cont.).

Inter-fraction (Setup error)						
Patient	LMT			LLT		
No.8						
Fraction	Vertical	Longitudinal	Lateral	Vertical	Longitudinal	Lateral
	(cm)	(cm)	(cm)	(cm)	(cm)	(cm)
21	0.0900	-0.0300	0.2000	-0.1100	0.1100	0.1400
22	-0.2600	0.2300	0.1400	0.1100	-0.0100	0.1000
Mean	-0.0593	0.0229	0.0436	-0.0222	0.0161	0.0217
SD	0.1309	0.1125	0.0748	0.0945	0.1178	0.0708

Table B.16 Data of intra fraction for individual patient No.8 in vertical, longitudinal and lateral directions using real- time 3D surface tracking system in breast cancer patient was treated with DIBH technique.

Intra- fraction (Patient movement)						
Patient	LMT			LLT		
No.8						
Fraction	Vertical	Longitudinal	Lateral	Vertical	Longitudinal	Lateral
	(cm)	(cm)	(cm)	(cm)	(cm)	(cm)
1	-0.0267	0.0400	0.0300	-0.043	0.005	0.020
2	-0.0300	0.0525	0.0275	0.008	-0.030	0.005
3	-0.0333	0.0200	0.0267	-0.007	-0.007	0.020
4	-0.0100	0.0025	0.0125	-0.046	0.036	0.034
5	-0.0200	-0.0100	0.0167	-0.005	0.015	0.010
6	-0.0140	-0.0080	0.0180	-0.077	0.043	0.023
7	-0.0400	-0.0167	0.0333	-0.085	0.028	-0.008
8	-0.0033	-0.0500	-0.0233	-0.130	0.018	-0.035
9	-0.0533	0.0233	0.0000	-0.093	0.028	0.000
10	-0.0300	0.0750	0.0950	0.025	0.008	0.017

Table B.16 Data of intra fraction for individual patient No.8 in vertical, longitudinal and lateral directions using real- time 3D surface tracking system in breast cancer patient was treated with DIBH technique (cont.).

Intra- fraction (Patient movement)						
Patient	LMT			LLT		
No.8						
Fraction	Vertical	Longitudinal	Lateral	Vertical	Longitudinal	Lateral
	(cm)	(cm)	(cm)	(cm)	(cm)	(cm)
11	-0.0040	0.0080	0.0040	-0.030	0.008	0.005
12	-0.0800	0.0240	0.0160	-0.008	-0.005	0.020
13	-0.0467	0.0167	-0.0067	-0.070	0.048	0.008
14	-0.0333	0.0067	0.0433	-0.057	0.020	0.017
15	-0.0033	0.0267	0.0100	-0.045	0.068	0.020
16	0.0225	-0.0050	0.0400	-0.013	0.003	0.023
17	-0.0600	0.0767	0.0033	-0.068	0.030	-0.003
18	-0.0100	0.0133	0.0133	0.015	0.068	0.093
19	-0.0620	0.0220	-0.0220	-0.053	0.085	0.013
20	-0.0200	0.0150	-0.0050	-0.045	0.053	-0.013
21	0.0300	0.0500	0.0233	0.003	0.015	0.020
22	0.0167	-0.0300	0.0000	-0.010	0.013	0.003
Mean	-0.0275	0.0127	0.0168	-0.0402	0.0267	0.0127
SD	0.0327	0.0313	0.0237	0.0389	0.0271	0.0224

Table B.17 Data of inter fraction for individual patient No.9 in vertical, longitudinal and lateral directions using real- time 3D surface tracking system in breast cancer patient was treated with DIBH technique

Inter-fraction (Setup error)						
Patient	LMT			LLT		
No.9						
Fraction	Vertical	Longitudinal	Lateral	Vertical	Longitudinal	Lateral
	(cm)	(cm)	(cm)	(cm)	(cm)	(cm)
1	-0.1300	-0.1500	-0.1400	-0.2300	-0.0900	-0.1200
2	-0.1100	0.0400	-0.1300	-0.1700	0.1300	-0.0900
3	0.0400	-0.0500	0.0200	0.0400	-0.0800	0.0100
4	-0.1400	-0.0500	-0.1600	-0.1000	0.0200	-0.1800
5	-0.0300	-0.1100	0.0400	-0.1100	-0.1000	0.0300
6	-0.0800	0.1400	-0.0900	-0.1100	0.0600	-0.1800
7	0.0200	-0.0900	-0.1600	0.0500	-0.1000	-0.1600
8	-0.1100	-0.1600	-0.2200	-0.0500	-0.2200	-0.2100
9	0.1900	0.0500	0.0000	0.1000	0.1400	0.0800
10	-0.1400	0.0900	0.1000	-0.0600	0.0000	0.0600
11	0.0600	0.2000	-0.0400	0.1300	0.1900	-0.0700
12	-0.0400	-0.0200	0.0300	-0.2000	0.1200	0.1000
13	-0.1200	-0.1100	0.0100	-0.2900	-0.0400	-0.0800
14	0.0000	0.1000	0.0000	-0.0100	0.0200	0.0000
15	0.0000	0.0000	0.0000	-0.1400	0.0000	-0.0200
16	0.0000	0.0300	0.0700	-0.0700	0.0500	0.0300
17	-0.0200	0.0400	0.0300	-0.0700	-0.0500	-0.0200
18	0.0300	0.0200	0.0600	-0.0400	0.0100	0.0100
19	-0.0400	0.0000	0.0100	-0.0700	0.0000	0.0100
20	-0.1000	0.0300	0.0600	-0.1900	0.0100	0.0100
21	-0.0800	0.0400	0.0400	-0.1600	0.0100	-0.0100
Mean	-0.0381	0.00190	-0.0224	-0.0833	0.0038	-0.0381
SD	0.0819	0.0930	0.0903	0.1070	0.0951	0.0897

Table B.18 Data of intra fraction for individual patient No.9 in vertical, longitudinal and lateral directions using real- time 3D surface tracking system in breast cancer patient was treated with DIBH technique.

Intra- fraction (Patient movement)						
Patient	LMT			LLT		
No.9						
Fraction	Vertical	Longitudinal	Lateral	Vertical	Longitudinal	Lateral
	(cm)	(cm)	(cm)	(cm)	(cm)	(cm)
1	0.0040	-0.0700	0.0000	-0.0050	0.0025	-0.0100
2	-0.0280	0.0320	0.0840	-0.0020	0.0020	0.0000
3	-0.0080	0.0080	-0.0080	-0.0340	0.0140	0.0020
4	-0.0060	-0.0280	-0.0060	-0.0040	-0.0320	0.0020
5	-0.0120	0.0280	0.0240	-0.0080	0.0160	0.0400
6	0.0160	0.0160	0.0200	0.0000	-0.0100	-0.0050
7	-0.0020	-0.0080	-0.0040	-0.0180	-0.0020	0.0000
8	-0.0020	0.0020	-0.0060	0.0000	0.0480	0.0300
9	-0.0260	-0.0160	-0.0260	-0.0150	0.0075	-0.0250
10	-0.0100	-0.0120	0.0060	-0.0180	0.0180	0.0100
11	0.0020	-0.0040	-0.0080	-0.0080	0.0220	0.0100
12	-0.0040	0.0240	0.0120	0.1200	-0.0750	-0.0125
13	-0.0500	0.0120	-0.0180	-0.1120	-0.0240	0.0060
14	-0.0020	-0.0900	-0.0020	0.0020	-0.0320	-0.0180
15	0.0180	0.0020	0.0000	-0.0580	0.0180	0.0040
16	-0.0180	-0.0120	-0.0060	0.0020	0.0760	0.0380
17	-0.0300	0.0040	-0.0020	-0.0060	0.0360	0.0100
18	-0.0025	0.0100	0.0125	0.0320	0.0020	0.0220
19	-0.0175	-0.0175	0.0150	-0.0080	0.0120	0.0200
20	-0.0075	-0.0175	0.0025	-0.0520	0.0020	-0.0100
Mean	-0.0093	-0.0069	0.0045	-0.0096	0.0051	0.0057
SD	0.0159	0.0300	0.0223	0.0426	0.0316	0.0176

Table B.19 Data of inter fraction for individual patient No.10 in vertical, longitudinal and lateral directions using real- time 3D surface tracking system in breast cancer patient was treated with DIBH technique.

Inter-fraction (Setup error)						
Patient	LMT			LLT		
No.10						
Fraction	Vertical	Longitudinal	Lateral	Vertical	Longitudinal	Lateral
	(cm)	(cm)	(cm)	(cm)	(cm)	(cm)
1	-0.2000	0.1000	0.0500	-0.2400	0.1700	-0.0500
2	0.0200	-0.0700	0.1600	-0.2900	0.3000	0.0400
3	-0.1400	0.2600	0.2400	-0.1100	0.2000	0.2800
4	0.0000	0.0600	0.1800	0.0500	0.0300	0.2700
5	-0.1000	0.1000	0.0400	-0.0200	0.0700	0.0300
6	-0.1800	0.0300	0.0300	-0.1000	-0.0300	0.0400
7	-0.1900	0.0100	0.0800	-0.2600	0.1200	0.1100
8	-0.1200	0.1300	0.1500	-0.0600	0.0600	0.2200
9	0.1500	-0.2200	-0.0300	0.1300	-0.1700	-0.0600
10	-0.1000	0.0600	0.2700	-0.1000	0.1100	0.3200
11	-0.2200	0.0600	0.1700	-0.2000	0.1200	0.1800
12	-0.3000	0.1300	0.3100	-0.1800	0.0700	0.2300
13	-0.2500	0.0300	-0.0900	-0.2300	0.0200	-0.0900
14	-0.1000	0.1500	0.1000	-0.0800	0.1600	0.1200
15	-0.0300	-0.0100	0.0600	-0.1000	0.1300	0.1700
Mean	-0.0958	0.0526	0.0984	-0.0858	0.0605	0.1000
SD	0.1272	0.1156	0.1133	0.1299	0.1153	0.1234

Table B.20 Data of intra fraction for individual patient No.10 in vertical, longitudinal and lateral directions using real- time 3D surface tracking system in breast cancer patient was treated with DIBH technique.

Intra- fraction (Patient movement)						
Patient	LMT			LLT		
No.10						
Fraction	Vertical	Longitudinal	Lateral	Vertical	Longitudinal	Lateral
	(cm)	(cm)	(cm)	(cm)	(cm)	(cm)
1	-0.0140	0.0640	0.0280	-0.0080	0.0640	0.0200
2	-0.0200	0.0160	-0.0100	0.0420	-0.0720	0.0240
3	-0.0280	-0.0020	0.0000	-0.0180	0.0660	-0.0180
4	-0.0460	0.0520	0.0040	-0.1360	0.2060	-0.0140
5	-0.0900	0.0880	0.0020	-0.1340	0.1560	0.0360
6	-0.0260	0.0520	0.0360	-0.0660	0.1160	0.0000
7	-0.0280	0.0380	-0.0240	0.0288	-0.0348	-0.0100
8	-0.0100	0.0300	0.0133	-0.0175	0.0300	-0.0025
9	-0.0440	0.0520	0.0260	-0.0425	0.0525	0.0050
10	-0.0800	0.0825	0.0325	-0.0100	-0.0400	-0.0150
11	0.0425	-0.0350	-0.0400	-0.0650	0.0600	0.0200
12	-0.0467	0.0633	0.0367	0.0550	-0.0800	0.0450
13	-0.0360	0.0920	0.0460	-0.0480	0.1740	0.0300
14	-0.0540	0.0660	-0.0160	-0.0940	0.1100	0.0280
15	-0.0460	0.0140	-0.1340	-0.0800	0.0600	0.0025
16	0.1640	-0.1800	0.1080	-0.0280	0.0440	-0.0040
17	-0.1000	0.1450	-0.0250	-0.1400	0.0820	-0.0040
18				-0.1100	0.1267	-0.0167
19				-0.1120	0.1660	0.0180
Mean	-0.0272	0.0375	0.0049	-0.0517	0.0677	0.0076
SD	0.0592	0.0694	0.0499	0.0601	0.0822	0.0194

Table B.21 Data of inter fraction for individual patient No.11 in vertical, longitudinal and lateral directions using real- time 3D surface tracking system in breast cancer patient was treated with DIBH technique.

Inter-fraction (Setup error)						
Patient	LMT			LLT		
No.11						
Fraction	Vertical	Longitudinal	Lateral	Vertical	Longitudinal	Lateral
	(cm)	(cm)	(cm)	(cm)	(cm)	(cm)
1	-0.1800	0.1200	0.0400	0.0100	-0.0900	0.0500
2	-0.0700	-0.1400	0.1500	-0.1000	0.1600	0.0600
3	0.1500	-0.1000	-0.0300	-0.0400	-0.0600	0.0000
4	0.0000	-0.1700	-0.0300	0.2400	-0.0200	0.1000
5	0.1600	0.0400	0.1100	-0.0400	0.0300	0.0900
6	0.1500	-0.0800	-0.0600	-0.1900	0.0800	0.0200
7	0.0800	-0.0800	0.0600	-0.1000	0.1200	0.0400
8	-0.1200	0.0600	0.0900	0.1200	0.0100	0.0400
9	-0.0400	-0.0100	-0.0800	-0.0300	-0.1800	0.1200
10	0.0900	0.0400	0.0200	-0.1200	-0.0900	-0.2400
11	-0.0100	-0.1300	0.1200	-0.0400	0.1000	0.1400
12	-0.1700	-0.0800	-0.1600	0.1900	-0.1000	-0.2700
13	-0.0700	-0.1100	-0.2400	0.0900	-0.1500	0.0300
14	0.0900	-0.0800	0.0900	0.1400	-0.0600	0.0300
15	-0.0600	0.2200	-0.2000	0.1500	-0.0900	0.0200
16	0.0800	0.0900	0.1000	0.0700	0.0600	0.2700
17	-0.0300	0.0200	0.0600	-0.2400	0.1600	0.3000
18	0.1000	-0.1000	-0.0200			
19	-0.0200	0.0200	-0.1400			
20	0.2100	-0.0900	0.2200			
21	-0.1100	-0.0500	0.1600			
Mean	0.0110	-0.0290	0.0124	0.0065	-0.0071	0.0471
SD	0.1130	0.0986	0.1245	0.1361	0.1068	0.1414

Table B.22 Data of intra fraction for individual patient No.11 in vertical, longitudinal and lateral directions using real- time 3D surface tracking system in breast cancer patient was treated with DIBH technique.

Intra- fraction (Patient movement)						
Patient	LMT			LLT		
No.11						
Fraction	Vertical	Longitudinal	Lateral	Vertical	Longitudinal	Lateral
	(cm)	(cm)	(cm)	(cm)	(cm)	(cm)
1	0.0100	-0.0150	0.0250	0.0050	0.0050	0.0200
2	-0.0067	0.0233	-0.0100	-0.0133	0.0100	0.0133
3	-0.0400	0.0200	0.0000	-0.0200	-0.0067	0.0033
4	-0.0167	0.0900	0.0100	-0.0100	0.0100	-0.0300
5	-0.0567	0.0633	0.0133	0.0033	0.0300	-0.0033
6	-0.0367	0.0267	0.0200	0.0200	-0.0033	0.0233
7	-0.0367	0.0333	-0.0100	-0.0300	0.0167	0.0033
8	-0.0033	-0.0300	-0.0133	0.0000	0.0033	0.0033
9	0.0100	-0.0233	0.0167	0.0067	0.0200	-0.0033
10	0.0067	0.0367	0.0267	-0.0267	-0.0100	0.0033
11	0.0167	-0.0033	0.0200	0.0050	0.0200	0.0300
12	0.0025	-0.0100	-0.0150	0.0000	0.0250	-0.0100
13	-0.0450	0.0350	-0.0200	0.0000	0.0033	-0.0233
14	-0.0067	0.0100	-0.0233	0.0067	-0.0267	0.0033
15	-0.0300	0.0100	-0.0150	-0.3233	0.2500	-0.2000
16	0.0033	-0.0200	0.0100	0.1333	-0.1233	-0.0600
17	0.0400	-0.0200	0.0200	0.0133	-0.0033	-0.0467
18	0.0333	0.0467	0.0333			
19	0.0067	-0.0033	-0.0100			
20	-0.0333	0.0200	-0.0133			
21	-0.0467	0.0433	-0.0167			
Mean	-0.0109	0.0159	0.0023	-0.0135	0.0129	-0.0161
SD	0.0273	0.0311	0.0181	0.0874	0.0701	0.0530

Table B.23 Calculated SD of mean for interfraction for population in vertical, longitudinal and lateral direction of LMT and LLT field for eleven patients.

Mean of Interfraction						
Field	LMT			LLT		
Patient No.	Vertical (cm)	Longitudinal (cm)	Lateral (cm)	Vertical (cm)	Longitudinal (cm)	Lateral (cm)
1	0.0041	-0.0606	-0.0218	-0.0294	-0.0406	-0.0600
2	-0.0456	0.0180	0.0100	-0.0763	-0.0088	-0.0017
3	-0.0305	0.0143	0.0386	-0.0220	0.0085	0.0815
4	0.0114	-0.0364	0.0393	-0.0977	0.0531	0.0492
5	-0.0300	-0.0450	0.0479	-0.0640	-0.0333	0.0400
6	0.0268	0.0368	0.1074	0.0005	0.0211	0.0895
7	-0.0577	0.0400	0.0055	-0.0229	0.0282	-0.0271
8	-0.0593	0.0229	0.0436	-0.0222	0.0161	0.0217
9	-0.0381	0.0019	-0.0224	-0.0833	0.0038	-0.0381
10	-0.0958	0.0526	0.0984	-0.0858	0.0605	0.1000
11	0.0110	-0.0290	0.0124	0.0065	-0.0071	0.0471
SD of Mean	0.0374	0.0382	0.0424	0.0371	0.0318	0.0519

Table B.24 Calculated SD of mean for intrafraction for population in vertical, longitudinal and lateral direction of LMT and LLT field for eleven patients.

Mean of Intrafraction						
Field	LMT			LLT		
Patient No.	Vertical (cm)	Longitudinal (cm)	Lateral (cm)	Vertical (cm)	Longitudinal (cm)	Lateral (cm)
1	-0.0392	0.0444	0.0127	-0.0482	0.0469	0.0123
2	-0.0059	-0.0061	-0.0194	0.0019	-0.0080	-0.0077
3	-0.0406	0.0430	-0.0076	-0.0632	0.0440	-0.0050
4	-0.0523	0.0421	-0.0063	-0.0072	0.0117	-0.0072
5	0.0065	0.0149	0.0124	0.0122	-0.0629	0.0089

Table B.24 Calculated SD of mean for intrafraction for population in vertical, longitudinal and lateral direction of LMT and LLT field for eleven patients (conts).

Mean of Intrafraction						
Field	LMT			LLT		
Patient No.	Vertical (cm)	Longitudinal (cm)	Lateral (cm)	Vertical (cm)	Longitudinal (cm)	Lateral (cm)
6	-0.0254	0.0224	0.0132	0.0089	-0.0173	0.0068
7	0.0130	-0.0058	-0.0149	-0.0125	0.0018	-0.0072
8	-0.0275	0.0127	0.0168	-0.0402	0.0267	0.0127
9	-0.0093	-0.0069	0.0045	-0.0096	0.0051	0.0057
10	-0.0272	0.0375	0.0049	-0.0517	0.0677	0.0076
11	-0.0109	0.0159	0.0023	-0.0135	0.0129	-0.0161
SD of Mean	0.0204	0.0202	0.0122	0.0261	0.0355	0.0098

Table B.25 Calculated mean of SD for interfraction for population in vertical, longitudinal and lateral direction of LMT and LLT field for eleven patients.

SD of Interfraction						
Field	LMT			LLT		
Patient No.	Vertical (cm)	Longitudinal (cm)	Lateral (cm)	Vertical (cm)	Longitudinal (cm)	Lateral (cm)
1	0.1142	0.1195	0.1312	0.0906	0.1138	0.1629
2	0.1161	0.1019	0.1202	0.1187	0.1330	0.1433
3	0.0917	0.1013	0.0659	0.0963	0.1171	0.1015
4	0.0972	0.1679	0.1254	0.0971	0.1079	0.1154
5	0.0991	0.0804	0.1141	0.0991	0.0884	0.1225
6	0.1257	0.1149	0.1184	0.1380	0.1474	0.1358
7	0.1386	0.0985	0.0919	0.0889	0.0869	0.0917
8	0.1309	0.1125	0.0748	0.0945	0.1178	0.0708
9	0.0819	0.0930	0.0903	0.1070	0.0951	0.0897
10	0.1272	0.1156	0.1133	0.1299	0.1153	0.1234

Table B.25 Calculated mean of SD for interfraction for population in vertical, longitudinal and lateral direction of LMT and LLT field for eleven patients (cont.).

SD of Interfraction						
Field	LMT			LLT		
Patient No.	Vertical (cm)	Longitudinal (cm)	Lateral (cm)	Vertical (cm)	Longitudinal (cm)	Lateral (cm)
11	0.1130	0.0986	0.1245	0.1361	0.1068	0.1414
Mean of SD	0.1123	0.1095	0.1064	0.1087	0.1118	0.1180

Table B.26 Calculated mean of SD for intrafraction for population in vertical, longitudinal and lateral direction of LMT and LLT field for eleven patients.

SD of Intrafraction						
Field	LMT			LLT		
Patient No.	Vertical (cm)	Longitudinal (cm)	Lateral (cm)	Vertical (cm)	Longitudinal (cm)	Lateral (cm)
1	0.0371	0.0352	0.0171	0.0465	0.0403	0.0367
2	0.0475	0.0578	0.0481	0.0379	0.0371	0.0341
3	0.0293	0.0238	0.0469	0.0752	0.0289	0.0226
4	0.0965	0.0906	0.0308	0.0220	0.0280	0.0201
5	0.0259	0.0320	0.0208	0.0192	0.2074	0.0244
6	0.0917	0.0873	0.0462	0.0427	0.1288	0.0262
7	0.0749	0.0751	0.0287	0.0345	0.0200	0.0394
8	0.0327	0.0313	0.0237	0.0389	0.0271	0.0224
9	0.0159	0.0300	0.0223	0.0426	0.0316	0.0176
10	0.0592	0.0694	0.0499	0.0601	0.0822	0.0194
11	0.0273	0.0311	0.0181	0.0874	0.0701	0.0530
Mean of SD	0.0489	0.0512	0.0320	0.0461	0.0638	0.0287

BIOGRAPHY

NAME	Mr.Jaruek Kanphet
DATE OF BIRTH	25 May 1982
PLACE OF BIRTH	Prachinburi, Thailand
INSTITUTIONS ATTENDED	Mahidol University, 2005 Bachelor of Science (Radiological Technology) Thammasat University, 2011 Bachelor of Law Mahidol University, 2016 Master of Science (Medical Physics)
HOME ADDRESS	20/869 Nonsri Road, Chongnonsri, Yannawa, Bangkok, Thailand Tel. +66-81-934-3386 E-mail : jaruek2525@gmail.com
EMPLOYMENT ADDRESS	King Chulalongkorn Memorial Hospital, 1873 Rama IV Road, Prathumwan, Bangkok, Thailand Tel. +66-2-256-4404